

Marshall University

Marshall Digital Scholar

---

Theses, Dissertations and Capstones

---

2022

## Spatially Controlled Monolayers for Electrically Switchable Biomolecule Detection

Eduard Likhmanov  
lukehdik@gmail.com

Follow this and additional works at: <https://mds.marshall.edu/etd>



Part of the [Biochemistry Commons](#), [Biotechnology Commons](#), [Molecular Biology Commons](#), and the [Other Biochemistry, Biophysics, and Structural Biology Commons](#)

---

### Recommended Citation

Likhmanov, Eduard, "Spatially Controlled Monolayers for Electrically Switchable Biomolecule Detection" (2022). *Theses, Dissertations and Capstones*. 1626.  
<https://mds.marshall.edu/etd/1626>

This Thesis is brought to you for free and open access by Marshall Digital Scholar. It has been accepted for inclusion in Theses, Dissertations and Capstones by an authorized administrator of Marshall Digital Scholar. For more information, please contact [zhangj@marshall.edu](mailto:zhangj@marshall.edu), [beachgr@marshall.edu](mailto:beachgr@marshall.edu).

**SPATIALLY CONTROLLED MONOLAYERS FOR ELECTRICALLY  
SWITCHABLE BIOMOLECULE DETECTION**

A thesis submitted to  
the Graduate College of  
Marshall University  
In partial fulfillment of  
the requirements for the degree of  
Master of Science

In  
Chemistry

by  
Eduard Likhmanov

Approved by  
Dr. Scott Day, Committee Chairperson  
Dr. Rosalynn Quiñones-Fernandez  
Dr. Michael Norton

Marshall University  
August 2022

## APPROVAL OF THESIS

We, the faculty supervising the work of Eduard Likhmanov, affirm that the thesis, *Spatially Controlled Monolayers for Electrically Switchable Biomolecule Detection*, meets the high academic standards for original scholarship and creative work established by the Master of Science in Chemistry and the College of Science. This work also conforms to the editorial standards of our discipline and the Graduate College of Marshall University. With our signatures, we approve the manuscript for publication.



Dr. B. Scott Day, Department of Chemistry

Committee Chairperson

8/2/2022

Date



Dr. Michael Norton, Department of Chemistry

Committee Member

8/2/2022

Date



Dr. Rosalynn Quiñones, Department of Chemistry

Committee Member

8/2/2022

Date

© 2022  
Eduard Likhmanov  
ALL RIGHTS RESERVED

## Acknowledgments

I would like to start by thanking the people in my life who have provided infinite support throughout my entire career as a master's student here at Marshall. Without the unwavering belief and confidence in me of my loving mom Elena Aksenova and dad Igor Lukhmanov, as well as my optimistic and encouraging wife and eternal soulmate Jamie Lukhmanov, I would not be where I am today. From the bottom of my heart and soul, Thank You!

Secondly, I would like to say thank you to my research advisor and academic mentor, Dr. Scott Day. I am lucky to have worked with you for five long and hard (mostly, for you) years. You have inspired me in more ways than you can imagine from the day I met you. You have been there ready to give advice and guide me every time I needed anything, whether it was academic-related or not, and for that, you have my everlasting gratitude and respect.

Special thanks and honorable mentions go out to Dr. Michael Norton and David Neff, whose help along the way with every possible instrument or experiment cannot and will not be understated; to Elaine Martino for every little bit of extra support that I ever needed and for our deep conversations just about everything; to Stacy Good for being absolutely amazing at everything you do for this department and all the people in it, including students like me – without you we would all be lost in the ongoing chaos that is chemistry department's and Marshall's daily existence. Huge thanks to literally every single member of the chemistry department – I have met and had the honor and pleasure of studying for/working with/knowing some of the best examples of respectful and enjoyable professionals because of being a part of this department, and it helped me develop as a person I am today.

Last but definitely not least, a shoutout to all of my friends: long-distance friends from the past life half a world away who shall remain unnamed for the sake of not having to write a literal paragraph worth of names, friends I have made living here for eight years, and some of the best friends whom I have met through my chemistry journey at Marshall – Marcus White (aka “Dr. White”), Nathan Shin (aka “Wildest Hairstyle Nominee”), Yiannakis Lysandrou (aka “Bean Boy”), and Dylan Carpenter (aka “Mr. Mayor”). Without all of you, I would not have survived to become the person and friend that I strive to continue being today. Thank You!

## Table of Contents

Title.....	i
Approval of Thesis.....	ii
Copyright Page.....	iii
Acknowledgments.....	iv
Table of Contents.....	v-vi
List of Figures.....	vii-x
Abstract.....	xi
Introduction.....	1
Biological Sensors Background.....	1
Self-Assembled Monolayers Background.....	1
Hypothesis and Focus.....	5
Experimental.....	7
Materials.....	7
Dendron-DNA Conjugate Synthesis.....	8
Purification and Extraction of the Conjugates (Gel Electrophoresis).....	10
Surface and Conjugate Preparation for Conjugate Attachment.....	12
Polydimethylsiloxane (PDMS) Master Preparation and Microcontact Printing.....	13
Atomic Force Microscopy (AFM) Experiments.....	15
Surface Plasmon Resonance (SPR) Experiments.....	18
Results and Discussion.....	21
Dendron-DNA Conjugate Synthesis.....	21
Purification and Extraction of the Conjugates (Gel Electrophoresis).....	23
Surface and Conjugate Preparation for Conjugate Attachment.....	27
Polydimethylsiloxane (PDMS) Master Preparation and Microcontact Printing.....	32
Atomic Force Microscopy (AFM) Experiments.....	34
Surface Plasmon Resonance (SPR) Experiments.....	40

Summary .....	45
Future Work .....	46
References .....	48
Appendix A: Approval Letter .....	50
Appendix B: SPR Multi-Injection Peak Analysis .....	51

## List of Figures

- Figure 1.** A schematic diagram of an ideal, single-crystalline SAM of alkanethiolates supported on a gold surface. The general anatomy and characteristics of the SAM are highlighted.....3
- Figure 2.** An image showing idealized representation of the transition between straight (capturing) and bent (non-capturing) molecular conformations. This conformational change was originally inspired by Lahann et. al<sup>5</sup> and their work on switchable SAMs for the start of the study on the switchability of the designed G4 PAMAM switchable SAM. In this study, a bulky head group was used vs a bulky tail group, and the designed tail’s own properties were used to control potential switchability without the use of any additional ligands at the end. ....4
- Figure 3.** Dendron-maleimide-DNA conjugate synthesis. Step 1 shown in (a) is referred to as functionalization and serves the purpose of providing masked thiols for later attachment to gold. Step 2 illustrated in (b) is cleaving the dendrimer to produce functionalized dendrons, which will serve as the “heads” for gold attachment. Step 3 shown in (c) is maleimide-activation of ssDNA (18 bases) to provide a site for Michael addition of the functionalized dendron; these serve as “tails” of the conjugates. Step 4 illustrated in (d) is the Michael addition of functionalized cleaved dendron to the maleimide-activated DNA; these are the complete conjugates with masked thiols. ....8
- Figure 4.** Step-by-step diafiltration procedure that is utilized during multiple reactions of the synthesis as well as during the buffer substitution prior to and after the extraction via the gel electrophoresis. ....9
- Figure 5.** The final step of the conjugate synthesis, which unmask all sulfhydryls and is therefore completed just before the conjugates are to be put onto the gold for self-assembly.....12
- Figure 6.** A modified diagram adapted from Whitesides et al.<sup>8,9</sup> showing the multistep procedure that comprises PDMS master preparation and microcontact printing of the “ink” of choice onto gold. ....14
- Figure 7.** An image showing an EMF gold surface mounted on an AFM disk .....15



**Figure 8.** MultiMode Scanning Probe Microscope (SPM) Components. To the left, in (a), there is an SEM image of the cantilever and the tip. In the center, in (b) (top), the “head” of the microscope is shown; this is where the sample is inserted and where the position of the cantilever (and the tip), laser, and photodiode can all be adjusted. Under that, the piezoelectrical device and its idealized rastering pattern are illustrated. To the right, in (c), the microscope itself and the controller can be seen.....16

**Figure 9.** MM8 SPM alongside the full setup for the described electric potential switching experiments. To the left, in (a), there is a picture of the full setup with all electrodes connected, forming a closed circuit. To the right, in (b), is an image of the close-up look on the head of the MM8 SPM instrument with the gold surface with the wire connected mounted. Sticking out and down is the working electrode (black clip). Connected to the red clip is the auxiliary electrode, which is in contact with the water on the gold surface through the almost transparent tubing. In the middle, the gray wiring is the reference electrode, which is also in contact with the solution on the gold surface. On top of the gold is the AFM cell for liquid experiments. ....17

**Figure 10.** A diagram adapted from the BI-2000 SPR system user’s manual.<sup>10</sup> In the case of an SPR instrument, the light causing the resonance of surface plasmons is a laser which is incident upon the metal film. The SPR instrument is subjected to injections of molecules of study and is responsible for the detection of attachment or absence thereof by monitoring the angular shift of reflected light over time. ....18

**Figure 11.** An image of the actual setup of the BI 2000 SPR system used in this research with labeled positions for the components of the instrument. ....20

**Figure 12.** UV images of the EtBr-stained 4% agarose gels after gel electrophoresis of the G4 conjugates. This is done to extract the product from the unreacted starting materials and extraneous chemicals and purify them. The three UV images illustrated show the outcome of the same gel done for the G4 conjugate product purification and extraction. Images on the left (a) and right (b) differ only in their exposure level, while the one in the center (c) illustrates an actual gel piece cutout that was excised from the entire gel. ....26

**Figure 13.** NanoDrop™ 1000 spectrophotometer plots of the nucleotide absorbance values at various wavelengths. The cursor at 260 nm is indicative of one of the peaks where the absorbance is observed for the present nucleotides of the aliquot loaded into the instrument. There are two total peaks that are used to quantitate the present ssDNA, but the peak at 280 nm more or less becomes part of the peak at 260 nm due to its higher absorbance value. In (a) values for the absorbance prior to purification and extraction procedure is shown, and in (b) values for the absorbance at the same peaks after the purification and extraction procedure is illustrated. .27

**Figure 14.** Camera and AFM images showing the physical abrasions and unwanted materials being present on a surface that had undergone the designed cleaning procedure described previously.....28

**Figure 15.** SEM images of the bare CA134 EMF evaporated Cr/Au surface after the cleaning procedure at 20kV acceleration voltage, probe current of 12, working distance of 10 mm, and the magnifications of 35 (a), 1000 (b), and 10000 (c) collected through the JEOL Scanning Microscope 7200FLV (JSM7200). These images show uniformity of gold throughout the surface except for the couple of physical features seen in the first image – conducting tape and a single physical abrasion. The slight discoloration of the surface in the following two images is due to the conduction of several SEM scans completed on the single studied surface and saturation of the gold with the electrons from electron beam of the JSM7200. ....29

**Figure 16.** AFM image of the bare CA134 EMF evaporated Cr/Au surface (new) after the cleaning procedure collected through the MM8 SPM. The parameters for this scanned image were as follows: 50 µm scan size, 0.75 Hz frequency of oscillation of the cantilever with the tip, and 1024 scans per line. The dot(s) appearing blue are masked regions that are either remnants of limited physical abrasion on the surface or imaging artifacts.....29

**Figure 17.** The pitch of the TGG1 (manufacturer’s identifying number for the AFM grating) pattern on the silicon wafer.....33

**Figure 18.** Optical images of (a) a piece of silicon wafer with the pattern of interest on it. (b) the same piece of silicon wafer sitting next to the PDMS master produced from it following the procedure described previously. (c) The PDMS master that has been used all throughout this research that was produced from the TGG1 grating on the silicon wafer also in accordance with the aforementioned procedure for PDMS master preparation. ....34

**Figure 19.** An AFM image of the gold surface that had been microcontact-printed with HDT and backfilled with deacetylated SATP-functionalized G4 dendrimers (white lines) in (a). The individual grains are either removed by performing Laplace interpolation (blurry) or masking them (dark blue) in Gwyddion software. In (b), these are extracted height profiles that reflect data under the highlighted three lines in (a) visible on the gold surface. Gwyddion averages the values under lines and provides a convenient output that can be analyzed further on a peak-by-peak basis.....36

**Figure 20.** An AFM image of the gold surface that had been microcontact-printed with MCH and backfilled with deacetylated G4 conjugates (white lines) in (a). The individual grains and scars are masked (dark blue) in Gwyddion software. In (b), these are extracted height profiles that reflect data under the highlighted three lines in (a) visible on the gold surface. ....37

**Figure 21.** An AFM image from a liquid scan of the gold surface that had been microcontact-printed with MCH and backfilled with the designed SAM (white lines) in (a). The individual grains and scars are masked (dark blue) in Gwyddion software. In (b), these are extracted height profiles that reflect data under the highlighted four lines in (a) visible on the gold surface. ....38

**Figure 22.** An example image of a day’s worth of SPR experiments. Multiple injections are illustrated and labeled accordingly. The first two injections were G4 conjugate injections. Injections 3 and 4 included introducing 10  $\mu$ M Biotinylated Complementary DNA to the SAM on the gold. Injections 5 and 6 consisted of adding 10  $\mu$ M Streptavidin each time to the SAM with the complementary biotinylated DNA attached for the biomolecule detection testing. Lastly, injection 7 was 5 mM NaOH to disassemble the DNA double helix and leave just the SAM on the surface. This last injection is done so that the system can be used again for the same injections of biotinylated DNA followed by streptavidin to support reproducibility of biomolecular detection capabilities of the designed G4 SAM. The zoomed in and broken-down version of each peak can be found in Appendix B: SPR Multi-Injection peak breakdown. ....44

## **Abstract**

The development of biosensors that are low-waste, highly stable, and possess an ability to be interchanged between capturing and non-capturing configurations is promising for the biodetector field. Stable packing and attachment of the sensor, the ability to create an interchangeable detecting probe of interest relatively easily, and dynamic control of the probe via a reversible bias can provide for that. With the set goals to control all those properties, DNA-dendron conjugate molecules were designed, synthesized in solution, purified, and utilized to make self-assembled monolayers of single-stranded DNA on gold. To be able to manipulate the conjugates' sensing qualities in the described manners, generation 4 (G4) polyamidoamine dendrimers were conjugated to ssDNA oligomers (18 bases) in a one-to-one ratio and functionalized to provide multiple thiol groups for possible surface assembly. DNA-dendron successful conjugation and their purification were confirmed by using gel electrophoresis. The height profiles and dynamic switchability were tested by utilizing atomic force microscopy. The conjugates' attachment, packing density, and sensing ability were all measured from surface plasmon resonance experiments. The results outlined in this study demonstrate the potential of these novel DNA-dendron conjugates to advance the biosensors field and introduce a new way of thinking about the manufacturing of DNA monolayers on gold substrates.

## **Introduction**

### *Biological Sensors Background*

Biosensing devices are analytical devices that convert a biological response from a designed experimental system into an electrical signal that can be further analyzed to obtain desired results. Biosensors have many applications in fields such as food processing, monitoring, authenticity, quality and safety, fermentation processes, fluorescence imaging, biomedical field, military biodefense field, metabolic engineering, and plant biology, which makes them an invaluable resource in almost any job or aspect of life. When choosing a biodetecting device, the parameters that should be considered are high specificity, the relative independence of physical parameters such as pH and temperature, and, ideally, they should be potentially recyclable and usable more than once. Engineering, chemistry, and biology fields must all work together to develop the materials, transducing devices, and immobilization techniques needed to create good biosensors.<sup>1</sup>

Due to the required scientific research for the development of specific, pH and temperature-independent, and reusable biosensors, their current prices range from \$1000 to \$5000 in addition to the price of the laboratory equipment. Additionally, the market for biosensors is ever-growing, and each year it has been estimated to increase by approximately 7-8%.<sup>2</sup>

### *Self-Assembled Monolayers Background*

The molecular-level structure of a material defines the chemical and physical properties that the interface of the material will possess and show. Those properties can be affected or changed if the surface of the interface was tampered with, or, in other words, its composition was changed. One of the most common ways to alter the surface's properties is to attach other molecules to it.

Self-assembled monolayers (SAMs) are molecules that, when exposed to a metal or metal oxide surface, can adsorb to it.<sup>3</sup> This allows for two things: lowering of the free energy of the surface that the SAM is attached to and its surrounding environment and changing the surface's interfacial chemical and physical properties.<sup>4</sup> Self-assembling molecules bind to the surface with one end, the head group, and leave another end, the tail group, freely protruding away from the interface. Surface properties are tailored by the selection of molecules, particularly, the tail group, and the head group selection is usually determined by the material of the substrate.

Single-stranded DNA-based probes have seen an increase in their research and use over the last few decades due to several reasons such as their wide range of applications, the DNA's relative availability, and ease of modification. Some applications of the substrates produced by immobilizing ssDNA on the surface via SAMs include DNA sequencing, genetic disease diagnostics, gene profiling, simultaneous detection of DNA and antibodies, directed assembly of proteins, as well as detection of target analytes that include but are not limited to a multitude of biological molecules.<sup>5,6</sup> The aforementioned applications are achieved by attaching the conjugated ssDNA to a variety of substrates such as gold, silver, copper, palladium, platinum, and mercury. Among these substrates, gold is the most well-studied and commonly used. While there are many ways to tether ssDNA itself to the gold, the most common one is through using ssDNA molecules terminated with thiols, as they allow for the ready formation of the SAMs on the surface due to sulfur's naturally strong affinity for gold.<sup>3</sup>

SAMs have seen widespread applications since their creation in the late 1980s. Simple SAMs of single molecules have been applied to many surfaces including precious metals, metal oxides, and silicon oxide to name just a few.<sup>3</sup> Most monolayers are constructed from organic molecules that permit the user to change the physical and/or chemical properties of the interface.<sup>3</sup>

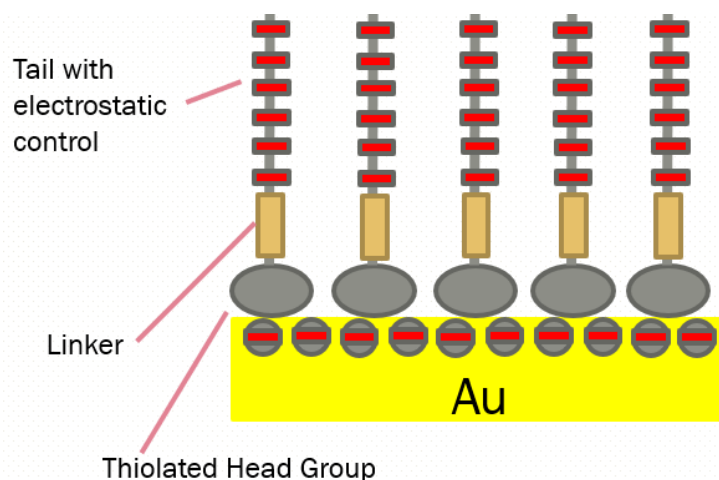


**Figure 1.** A schematic diagram of an ideal, single-crystalline SAM of alkanethiolates supported on a gold surface. The general anatomy and characteristics of the SAM are highlighted.

Since the original work of Love et al. that made a switchable wetting surface from alkanethiols on gold, stimuli-responsive surfaces have emerged as a new class of monolayers with an array of possible applications.<sup>3</sup> In these systems, monolayers are designed such that they exhibit two unique properties that are switched by an external stimulus that may include electric and magnetic fields, pH changes, reduction-oxidation reactions, and photonic stimulation.<sup>3</sup>

Different switchable SAMs have been studied throughout the years, but they share two things in common: they consist of what are referred to as the head group that is responsible for attachment of the molecule to the surface and a tail group that provides the surface with its newly affected properties, and they are capable of switching back and forth between conformations to either alter the surface's properties. There are a lot of different head and tail groups that could be and have already been studied; some of the examples of head groups include alcohols, diols, carboxylic acids, primary amines, and even cyanides, whereas the tails are generally constituted of varying alkyl chains or combinations thereof.<sup>3</sup> However, in this research, the head group studied was the dendron of the generation 4 (G4) polyamidoamine (PAMAM) dendrimer with free alkanethiols on its periphery, and the tail group was 5'-amine-modified single-stranded DNA.

Thiols are the most common head groups that are researched while studying SAMs due to the strong gold-thiol bond and the availability of the materials.<sup>3</sup>

Switchability of the SAMs is a relatively new aspect of SAMs that has been studied more recently. This acquired property of SAMs allows for the ability to “dynamically control” the interfacial properties of the surface that the SAMs are attached to through some kind of stimulus directed at the SAMs.<sup>5</sup> Stimuli may include alternating the solvent exposed to the surface with the SAM, changing the temperature of the surface, or applying an electrical field to the surface to alter its conformation for protruding ends of the SAM.<sup>5</sup> The latter method was chosen to be the affecting factor for this particular SAM. However, in order to attain the wanted switchability of the SAM, multiple requirements have to be fulfilled by the SAM’s structure. Among the requirements are a robust attachment to the surface, a low surface packing density throughout the monolayer, flexibility of the SAM’s molecular chain, and an ionizable functional group on the end of the SAM’s molecules.

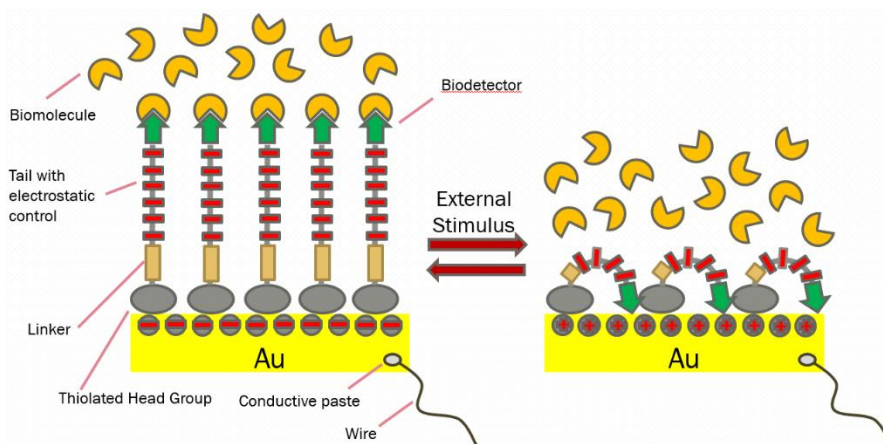


**Figure 2.** An image showing idealized representation of the transition between straight (capturing) and bent (non-capturing) molecular conformations. This conformational change was originally inspired by Lahann et. al<sup>5</sup> and their work on switchable SAMs for the start of the study on the switchability of the designed G4 PAMAM switchable SAM. In this study, a bulky head group was used vs a bulky tail group, and the designed tail’s own properties were used to control potential switchability without the use of any additional ligands at the end.



### *Hypothesis and Focus*

This research primary focused on optimizing the multi-step synthesis of the self-assembling molecules from varying maleimide-activated 5'-amine-modified single-stranded DNA molecules with 18 bases and a N-succinimidyl-S-acetylthiopropionate (SATP) functionalized G4 dendrimer that would then be used to coat a gold-coated glass surface to construct a switchable surface. The two main molecules that are listed above comprise the final conjugates that were self-assembled on the surface. The hypothesis is that the conjugates generated in this synthesis should satisfy all requirements for switchability. The multiple gold-thiol bonds of the dendrons allow for exceptionally robust attachment to the surface, the size of the dendron “footprint” provides a relatively low density for the required dynamic controllability of the SAM, and the long phosphate backbone of the attached maleimide-activated ssDNA provides flexibility and also allows ionizability.<sup>7</sup> The gold surface is important for this research because a conducting surface is needed for the switching of the surface under the applied electric field. The proposed change in conformations could potentially lead to the discovery of an affordable, relatively resistant, and reusable switching biosensor through observations of the known biotin/streptavidin protein interactions.

Another focus of this research was to utilize two techniques – Atomic Force Microscopy (AFM) and Fluorescence Microscopy – to verify switchability under the exposure of the substrate to external stimuli such as electric potential, observing two different properties – topography for AFM and fluorescence/quenching for fluorescence experiments. It is hypothesized that it would be possible to observe changes in the topographies of the two different conformations of the surfaces – one with SAMs’ tails protruding from the surface and one with the tails bent towards the surface – via utilizing the AFM experiments. As for fluorescence experiments, the

fluorescently-tagged DNA would be used in the synthesis of the proposed conjugates and, later, fluorescence signal quenching due to the proximity of the attached fluorophores to the gold substrate would be the property observed for confirmation of switching.

The last technique proposed to be used in this study is Surface Plasmon Resonance or SPR. With SPR, multiple aspects of this study are addressed that helped support the idea that the designed G4 SAM is able to switch between conformations and perform biosensing activity. Monitoring of self-assembly on gold, calculation of packing density, and SAM's ability to capture a pre-determined biomolecule of choice (streptavidin) by modifying the SAM slightly (biotinylating) were all accomplished during SPR and support this study's hypothesis.

## Experimental

### *Materials*

The materials that were used in this research are Generation 4 (G4) polyamidoamine (PAMAM) Dendrimers with a cystamine core acquired from Andrew ChemSciences, four unique DNA strands – 5'-amine-modified single-stranded DNA (5' Amino Modifier C6 with the 6 carbons between the modification and the DNA strand with the sequence of TAA CCA ATA GGC CGA AAT-3'), 5'-biotin-modified single-stranded DNA (5' Biotin Modifier is inserted integrally from an added dT base added to the AT TTC GGC CTA TTG GTT A-3' sequence at the 5' end), 5'-amine-modified 3'-biotin-modified single-stranded DNA (combines the two previously mentioned modifications and has a sequence of 5'-TAA CCA ATA GGC CGA AAT-3'), and unmodified single-stranded DNA with a sequence of 5'-AT TTC GGC CTA TTG GTT A-3' – all purchased from Integrated DNA Technologies. N-succinimidyl-S-acetylthiopropionate (SATP), sulfosuccinimidyl 4-[N-maleimidomethyl]cyclohexane-1-carboxylate (sSMCC), tris(2-carboxyethyl)phosphine hydrochloride (TCEP-HCl), and hydroxylamine were all purchased from Thermo Scientific. Hexadecanethiol (HDT), mercaptohexanol (MCH), and the line of gold wire were purchased from Sigma Aldrich. Milli-Q water ((distilled) water) used throughout the entire project was obtained from the Millipore Milli-Q lab water system purchased from Sigma Aldrich. Tris/acetic acid/EDTA (TAE) buffer was purchased from BIO-RAD. Analytical Grade Agarose, LE, was purchased from Promega Corporation. Ethidium Bromide (EtBr) was acquired from Fisher Bioreagents & Invitrogen. Silicon elastomer base and curing agent were purchased from Dow Corporation. Electrodag 5810 (EG 5810) two-component silver epoxy adhesive was purchased from Thorlabs. The silicon wafers were purchased from NT-MDT LLC, and the glass surfaces coated with gold were purchased from Evaporated Metal Films (EMF) (CA134) for AFM and Biosensing Instrument Inc. (BI) for SPR.

### Dendron-DNA Conjugate Synthesis

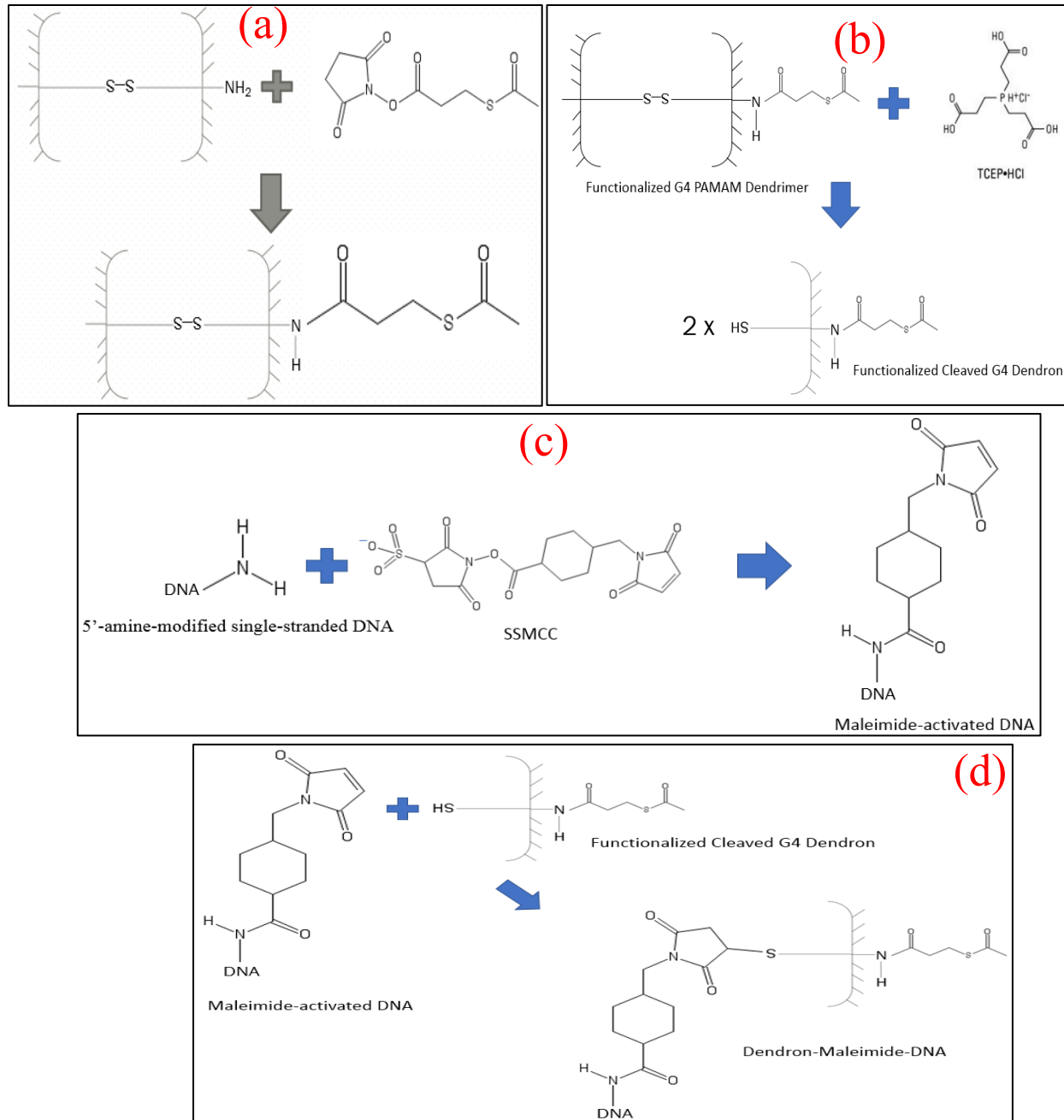


**Figure 3.** Dendron-maleimide-DNA conjugate synthesis. Step 1 shown in (a) is referred to as functionalization and serves the purpose of providing masked thiols for later attachment to gold. Step 2 illustrated in (b) is cleaving the dendrimer to produce functionalized dendrons, which will serve as the “heads” for gold attachment. Step 3 shown in (c) is maleimide-activation of ssDNA (18 bases) to provide a site for Michael addition of the functionalized dendron; these serve as “tails” of the conjugates. Step 4 illustrated in (d) is the Michael addition of functionalized, cleaved dendrons to the maleimide-activated DNA; these are the complete conjugates with masked thiols.

The initial step of this research was the multi-step synthesis of the proposed conjugates that are comprised of the dendron from Generation 4 PAMAM dendrimer and the maleimide-activated DNA molecule. The first reaction step in the synthesis involves fully dissolving enough SATP (1.25:1 molar ratio of SATP to each primary amine on the periphery of the dendrimer) in 20  $\mu$ L of DMSO, then diluting the solution to 190  $\mu$ L with 100 mM pH 7.2 phosphate buffered saline (PBS), and finally adding 10  $\mu$ L of ~6 mM G4 dendrimer to this solution in a single 1.5 mL plastic conical vial. This functionalization of the dendrimer via a nucleophilic substitution reaction of the primary amines of the G4 dendrimer and the NHS ester of the SATP (Figure 3 (a)) is given 45 minutes to 1 hour at room temperature (~23°C) to go to completion. This first reaction of the synthesis

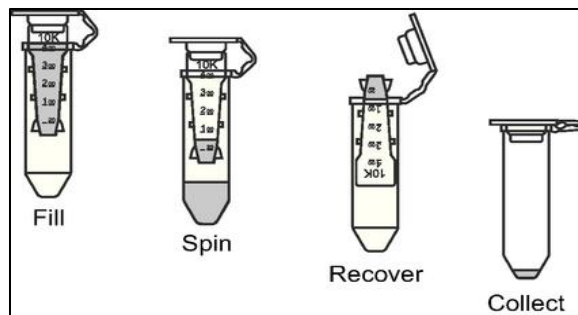


**Figure 4.** Step-by-step diafiltration procedure that is utilized during multiple reactions of the synthesis as well as during the buffer substitution prior to and after the extraction via the gel electrophoresis.

places thioacetate-protected thiol groups on each terminal end of the dendrimer periphery. Next, at the same time the dendrimer functionalization is started, the maleimide-activation of ssDNA is also initiated. This step involves fully dissolving enough sSMCC (2:1 molar ratio of sSMCC to ssDNA) in a 1.5 mL plastic conical vial in 20  $\mu$ L of DMSO, then adding pH 7.2 PBS to maintain as close pH as required by this reaction, and finally adding a number of  $\mu$ L of ssDNA required to make it a 1:3 molar ratio of ssDNA to dendron in the future reaction, making the total volume 500  $\mu$ L. This maleimide-activation of ssDNA via the addition of the primary amine on the ssDNA molecule to the maleimide of sSMCC (Figure 3 (c)) is given 1 hour at room temperature (~23°C) to proceed to completion. After the initial hour of the synthesis, solutions with both products are diafiltered by the utilization of the Amicon Ultra centrifugal filter devices with 3,000 nominal

molecular weight limit (NMWL) and 10,000 NMWL cutoffs for maleimide-activated DNA and functionalized dendrimers, respectively, using an Eppendorf MiniSpin Plus centrifuge for 30 and 7 minutes respectively, according to the technique illustrated in Figure 4. The cycle of diafiltration is done 2-3 times, depending on the molar ratio of SATP and sSMCC to the dendrimer and ssDNA for the respective reactions. Before the maleimide-activated DNA and the functionalized dendrimer are combined, the dendrimer must be cleaved into two dendrons by the reaction with TCEP that reduces the disulfide bond at the core, for which an amount that makes at least a 10:1 molar ratio of TCEP to dendrimer is weighed out and added directly to the tube with the now functionalized dendrimers. This reaction (Figure 3 (b)) is given 45 minutes to 1 hour at room temperature (~23°C) to go to completion. After the reaction with TCEP, the collected 50 µL of each functionalized and cleaved dendrons product and maleimide-activated DNA product are combined in a single clean tube; the volume is brought up to 200-300 µL to avoid potential solubility issues and allow for some space for the reaction to take place. This second to final chemical reaction (Figure 3 (d)) is given either overnight (~16-20 hours) at 4°C or 8 hours at room temperature (~23°C) to achieve maximum yield. The conjugated product is then purified and extracted with an agarose gel the next day.

#### *Purification and Extraction of the Conjugates (Gel Electrophoresis)*

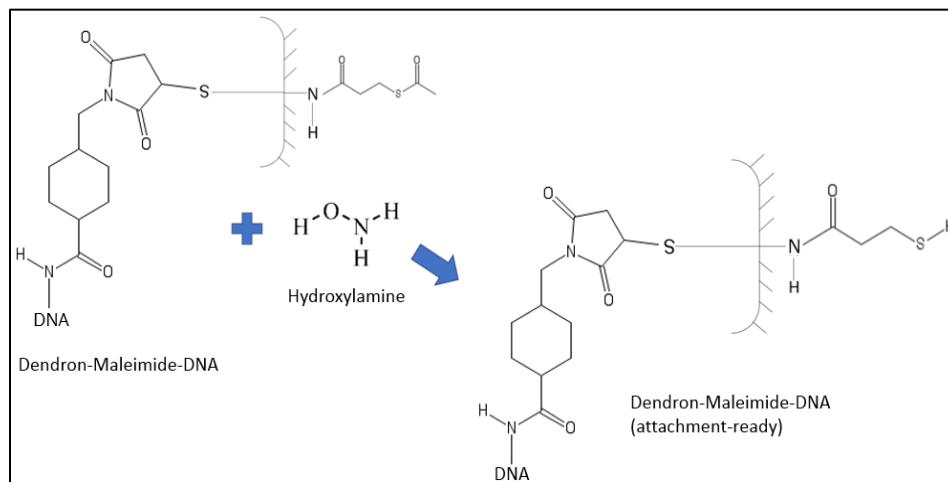
The process of getting the dendron-maleimide-DNA conjugates that have successfully reacted involves purification and extraction via gel electrophoresis. The gel (10 cm × 7 cm × 1 cm) is prepared by combining 2.8 g agarose and 70 mL of 1x TAE buffer, which makes it a 4% agarose gel. The choice of 4% was made due to the convenience of working with agarose versus polyacrylamide and ease of band excision from the gel. Additionally, ethidium bromide (7 µL of the 10000X solution per gel) is used as a means to visualize the ssDNA that is present in the gel.

The contents are put into an Erlenmeyer flask, heated up and mixed, then cooled to an appropriate temperature for the gel chamber (~34°C), poured into the chamber with a well-making comb, and allowed to set and harden for 1 hour. During this time, the conjugate solution is subjected to buffer substitution through 2-3 cycles of diafiltration that changes the PBS to 1x TAE buffer and rids the solution of extraneous TCEP, which interferes with the successful separation of the conjugates via gel electrophoresis, as was found throughout this research. Once the gel sets completely, the 1x TAE buffer is poured into the chamber, and the wells are loaded with conjugates to contain around the same amount of conjugate solution each, however many wells that takes. The gel is then run at 150 V for 30-35 minutes to allow for proper and complete separation of the conjugates from both the unreacted ssDNA and dendrons based on size difference between the two; the unreacted dendrimers (naturally slightly positive) are also separated away from the mix based on charge. After separation, an image of the gel is taken and used as a reference for the physical location of the conjugates in the gel. That location is then cut out from the gel via careful excision of the conjugate bands with a razor blade. The excised bands are cut/crushed and put into a 15 mL Falcon tube; enough 1x TAE buffer is added to cover the gel pieces and allow “sloshing around” when the tube is put on the rocker. The tube with the extraction buffer and gel pieces is put onto the rocker overnight to collect the purified product over the course of 16-20 hours. After the rocking, the solution is drawn in aliquots of 500  $\mu$ L and put into the 10000 NMWL Amicon Ultra centrifugal filter devices in order to concentrate the conjugates by the same process of diafiltration and collect them in a single tube. After the conjugates are concentrated, they are stored at 4°C in a refrigerator. NanoDrop<sup>TM</sup> 1000 spectrophotometer measurements are taken before the conjugates are loaded into the gel and after the entire purification process is complete; this is done to measure the yield of the whole reaction.

### *Surface and Conjugate Preparation for Conjugate Attachment*

The final chemical step of the conjugate synthesis is completed when the conjugates are used to prepare self-assembled monolayers on gold. Prior to putting the deacetylated conjugates on gold, a buffer substitution is done 2-3 times to exchange the buffer that the conjugates are dissolved in from 1x TAE (extraction buffer) to the pH 7.2 PBS reaction buffer; this is done through the same process of diafiltration described previously using the 10,000 NMWL Amicon Ultra centrifugal filter devices. Upon the completion of buffer substitution, the volume of the solution is brought up to ~150  $\mu$ L, and an amount of hydroxylamine is added to create at least a 2:1 molar ratio of hydroxylamine to thioacetate in the tube containing the conjugate solution. This reaction (Figure 5) is given 45 minutes to an hour to go to completion. In addition to hydroxylamine, some (~1 mg) TCEP is added to create a reducing environment in the solution to attempt prevention of any and all future possible disulfide bonds from forming among and within conjugates after the deprotection of the sulfhydryls. After the reaction is complete, the entire volume containing the conjugates that is present in the tube is transferred with a pipette directly onto a clean gold surface (patterned with HDT or MCH). The process of the conjugates' self-assembly is given overnight (~16 hours) or 3 hours (for faster experiment days) to go to completion.

**Figure 5.** The final step of the conjugate synthesis, which unmasks all sulfhydryls and is therefore completed just before the conjugates are to be put onto the gold for self-assembly.





During the final reaction of the synthesis, the EMF or BI gold surfaces are prepared, depending on the experimentation to follow afterward – AFM or SPR – accordingly. Both types of gold surfaces are cleaned the same way but come in different types and shapes, thusly requiring a little variation in the procedure for their preparation. Surfaces that are purchased from BI are ready to be cleaned as soon as they are unpacked from their box and respective slips, whereas EMF gold slides must be cut and broken off into approximately 1 cm<sup>2</sup> pieces due to the size limitation of the AFM sample stage. The cleaning procedure for both EMF and BI surfaces is the same and goes as follows: surfaces are taken out of their packaging and debris are removed by nitrogen gas flow, then, they are sonicated for 10-15 minutes in a beaker with enough isopropanol to cover, changing the solvent between cycles. Following sonication, the surfaces are dried with a stream of nitrogen gas once more and then plasma cleaned with air for 45-90 seconds using the Harrick Plasma PDC-32G plasma cleaner on high setting. In the case of AFM experiments, the surfaces undergo an additional step of preparation – gold wire attachment. This is required for the electric-potential-induced conjugates' switching experiments that are done during the completion of the AFM imaging experiments. To attach the wire directly to the gold surface, the EG 5810 epoxy is mixed in its' described component ratio (16 A : 1 B) on a glass slide, transferred in a small quantity (drop), and applied directly to the wire positioned on the gold surface. The surface with the epoxied wire is then cured in the 100°C oven for an hour. After the surface preparation procedures are complete, the surfaces are ready for either the optional microcontact printing and/or the deacetylated conjugate self-assembly.

#### *Polydimethylsiloxane (PDMS) Master Preparation and Microcontact Printing*

The PDMS master is prepared by combining the two parts – base and curing agent – in a 10:1 ratio by mass to make the PDMS master, and the viscous solution is degassed and poured

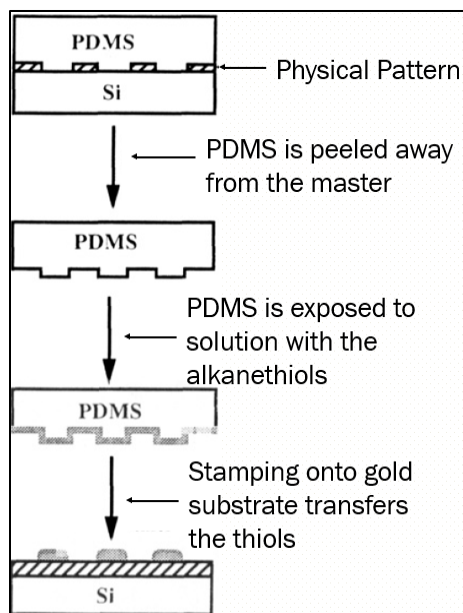


**Figure 6.** A modified diagram adapted from Whitesides et al.<sup>8, 9</sup> showing the multistep procedure that comprises PDMS master preparation and microcontact printing of the “ink” of choice onto gold.

over the silicon wafer with a pattern of interest (TGG1) placed into a small petri dish for convenience. Next, the solution is allowed to polymerize and harden overnight (~16 hours) in an 80°C oven. Then the master is cut out with a razor blade and cleaned by four 10-minute cycles of sonication using VWR Ultrasonic Cleaner – two in toluene and two in isopropanol – to rid the master of unpolymerized PDMS components and extraneous organic materials; it is also cleaned in the Harrick Plasma PDC-32G plasma

cleaner using air on the high setting for 30 seconds. The wafer and PDMS masters resulting from this process can be seen in Figure 6. Microcontact printing is done primarily with a 5 mM solution of hexadecanethiol (HDT) or 0.1 mM solution of mercaptohexanol (MCH) as “ink”, which are

both prepared in separate containers with ethanol in advance. Once the master is clean, the amount of “ink” that is enough solution (~25-30  $\mu\text{L}$ ) to cover the entire pattern is pipetted onto the master; the solution is allowed to “ink” the pattern for 30-60 seconds before it is blown off of the PDMS master with nitrogen while holding it securely. A clean gold surface is put into a petri dish, and then the PDMS master with “ink” is brought into contact with it, making sure the pattern is touching the gold by applying force to the four corners of the facedown PDMS master. The PDMS pattern only stays in contact with gold for 30-45 seconds, at which point it is withdrawn, taken off the gold, and the master is stored in its respective clean petri dish until the next microcontact printing. At this point, it is proposed that the gold is patterned with the “ink” and requires the

addition of the selected conjugates, which is done after their reaction with hydroxylamine for thiol deprotection. The exact used steps described in the procedure of both the preparation of the PDMS master and the microcontact printing were discovered and adapted from Kumar et al. and Xia and Whitesides.<sup>8,9</sup> The same PDMS master can be used many times without the need of making a new one by following the same cleaning procedure post-microcontact printing completion. The master that has been used for a single printing is put into a clean beaker and sonicated in ethanol or isopropanol or both for two to three cycles of ten minutes each. This ensures that any remaining “ink” is taken off the PDMS master, and that it is ready for the next time microcontact printing is used.

#### *Atomic Force Microscopy (AFM) Experiments*

Before starting the AFM experiments, the gold surface with the SAMs is checked to make sure there are no visible deposits of either salt from PBS or miscellaneous chemicals used throughout the synthesis; if there is anything visible, the surface is sonicated once or twice in Milli-Q distilled water for 5-15 minutes. Following sonication, the surface is dried with nitrogen and stored until measurements are made using AFM. The surface is then mounted on an AFM disk as shown in Figure 7 via double-sided tape for the entire time of the AFM experiment(s).

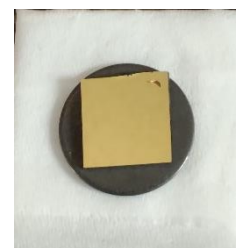


**Figure 7.** An image showing an EMF gold surface mounted on an AFM disk.

As for the experimentation part of the AFM itself, the MultiMode 8 (MM8) Scanning Probe Microscope (SPM) is the instrument that is used throughout this part, and its inner and outer components can be seen in Figure 8. The AFM scanning begins by making sure that the instrument is ready for use and sample loading: the computer, light source, and the controller of MM8 SPM are turned on, and only then is the sample loaded into the head of the MM8 SPM. The Nanoscope

software that allows for the collection of data is initiated as the sample is loaded in order to adjust the positioning of the sample live and find the exact area of interest. Once the area has been located and adjusted, the tip holder with the scanning tip of the type appropriate for the set of experiments being done (air or liquid AFM) is put on top of the sample with the tip being located way above the sample, at first. The sample location is adjusted to meet that of the tip and area of interest, the laser is focused on the cantilever, and scan parameters are modified to fit the needs of the experimental part (50  $\mu\text{m}$  scan size, 0.75 Hz frequency, 1024 sample size), and the sample is approached and engaged to begin the scan of the surface. The height profiles are collected and analyzed utilizing either the Nanoscope Analysis or Gwyddion software to level and process the AFM images.

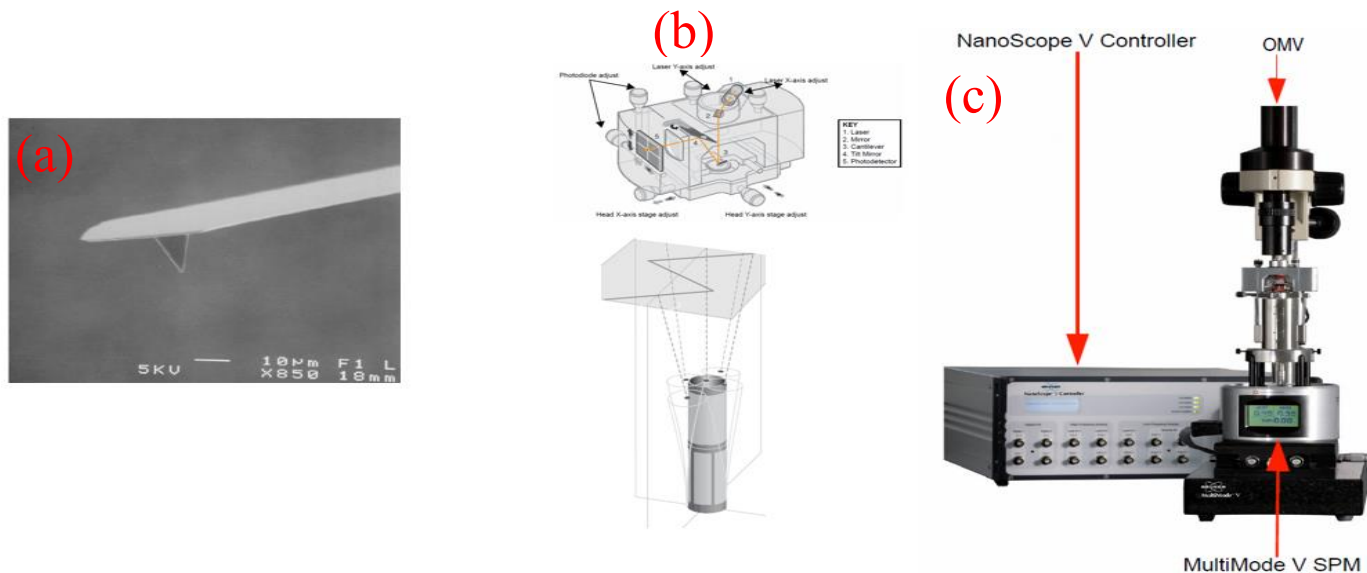


**Figure 8.** MultiMode Scanning Probe Microscope (SPM) Components. To the left, in (a), there is an SEM image of the cantilever and the tip. In the center, in (b) (top), the “head” of the microscope is shown; this is where the sample is inserted and where the position of the cantilever (and the tip), laser, and photodiode can all be adjusted. Under that, the piezoelectrical device and its idealized rastering pattern are illustrated. To the right, in (c), the microscope itself and the controller can be seen.

Throughout the collection of images during the AFM experiments, another aspect of this research is also addressed – the ability of the conjugates to switch between retracted and protruding

states of the SAMs' tails while on the surface and exposed to a reversible electrical bias, which is chosen to be the electric potential, in this case. Using the previously described attached wire, an electric potential of either a positive value of 0.3 volts (vs Ag/AgCl) or a negative value of the same magnitude is applied to the surface during the AFM scan(s) by utilizing the Bioanalytical Systems Inc. CV-27 Voltammograph. An example of the designed setup for this particular part is illustrated in Figure 9 below. In order to have a complete cell/circuit for the switching, the AFM scanning is in liquid (water), and the scans are collected one at a time: one scan in liquid with no potential applied, one scan for each positive/negative scenario, and one where the surface starts out with positive or negative potential applied to it and gets switched to the other mid-scan. All of these proposed scans should be able to illustrate the switching capabilities of the designed SAMs.

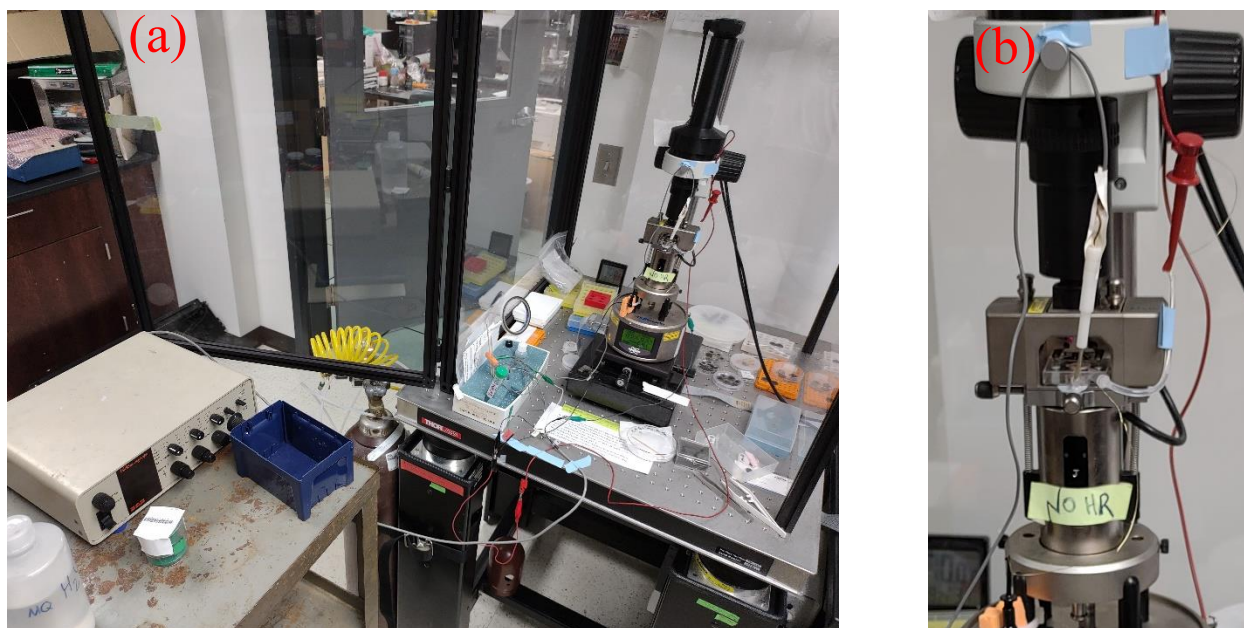


**Figure 9.** MM8 SPM alongside the full setup for the described electric potential switching experiments. To the left, in (a), there is a picture of the full setup with all electrodes connected, forming a closed circuit. To the right, in (b), is an image of the close-up look on the head of the MM8 SPM instrument with the gold surface with the wire connected mounted. Sticking out and down is the working electrode (black clip). Connected to the red clip is the auxiliary electrode, which is in contact with the water on the gold surface through the almost transparent tubing. In the middle, the gray wiring is the reference electrode, which is also in contact with the solution on the gold surface. On top of the gold is the AFM cell for liquid experiments.

### Surface Plasmon Resonance (SPR) Experiments

SPR works by using a thin metallic film in contact with a flow cell through which molecules are injected to form a monolayer on the film's surface. Metallic films are used because these films contain collections of free electrons, which will oscillate with respect to the metallic film. These collective oscillations of the free electrons in metallic films are called surface plasmons, and they resonate with light under the right conditions, causing absorption of light. This resonance condition is sensitive to the refractive index of the medium near the metallic film; therefore, the presence of molecules bound to the surface can be detected. The resonance angle

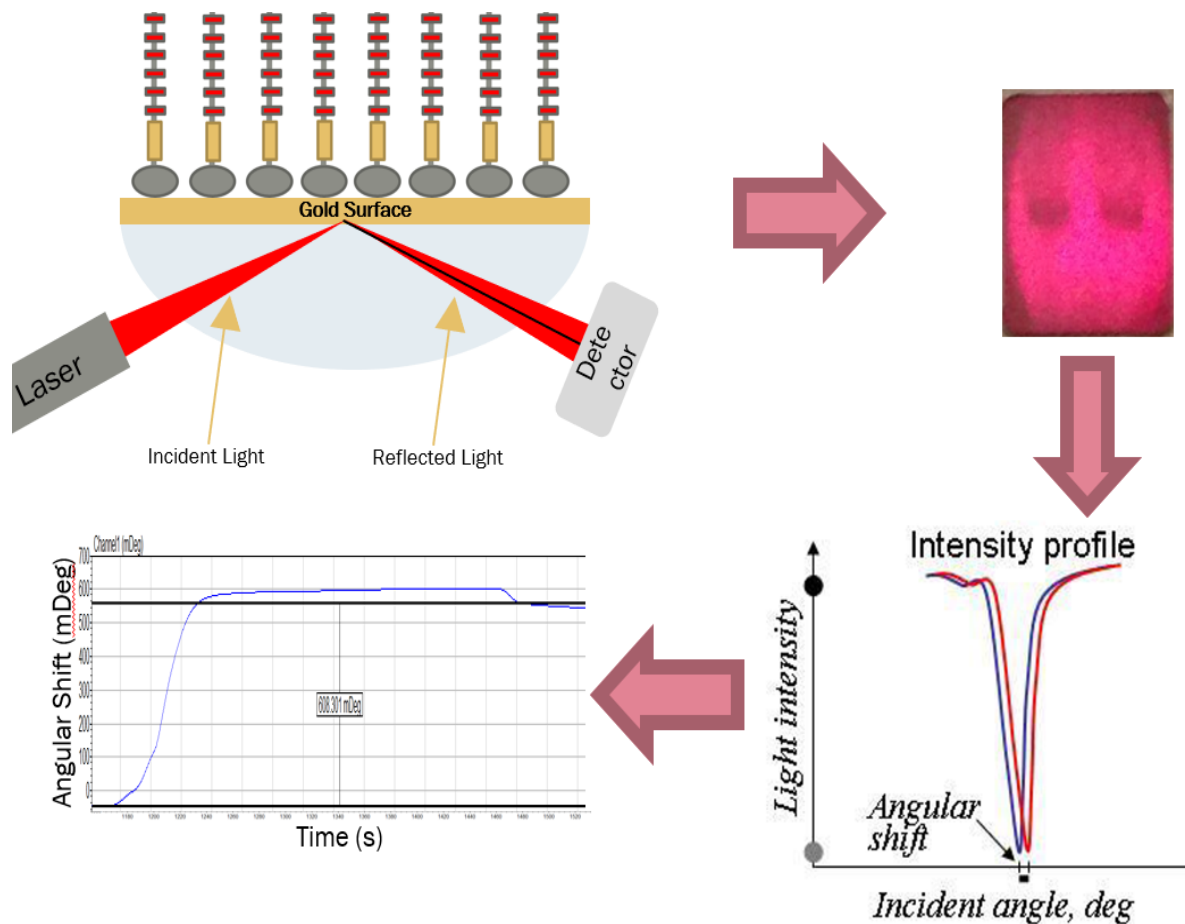


**Figure 10.** A diagram adapted from the BI-2000 SPR system user's manual.<sup>10</sup> In the case of an SPR instrument, the light causing the resonance of surface plasmons is a laser which is incident upon the metal film. The SPR instrument is subjected to injections of molecules of study and is responsible for the detection of attachment or absence thereof by monitoring the angular shift of reflected light over time.

causes a dip in the intensity of the laser light which shifts when molecules are added or desorbed from the surface, consequently allowing the molecules present on the surface to be measured. The instrument measures the angular shift in the light intensity caused by the molecules that are attached to or desorbed off the surface. And then the monitoring software produces a plot of that angular shift vs time.

The SPR instrument must be calibrated once in a while in order to ensure that the device is operating within the required/expected sensitivity range. Therefore, before loading and using any future working buffers, the system is flushed with and loaded with water and cleaned. Following that, the sensitivity is calibrated by using an ethanol solution of known concentration (1%) and gradually adjusting the software parameters to fit the ethanol calibration results in terms of injection time to allow for maximized interaction of analytes injected in the future. Ethanol (95%) and water are also the main liquids used for cleaning the inner workings/tubing of the SPR instrument.

Unlike the AFM experiments, there is no concern of any deposits prior to SPR experimentation, as the only procedure that had been followed with them is the cleaning by sonication and with plasma, due to the way the deposition of conjugates onto the surface is done during the actual SPR runs on the BI 2000 SPR system. The clean BI gold surface is mounted onto the matching fluid layer on top of the prism through which the laser shines onto the actual sample surface, and it is clamped down with the flow cell that has two channels. The channels are what the solutions flow through and come into contact with the surface to either be deposited (conjugates), attached to conjugates and detected (complementary DNA and/or target protein), or flow through with little to no interaction with the surface or SAMs (buffer). Due to the fact that there are two channels available for the flow of possible analytes or molecules that would interact

with them, two sets of data can be collected during the same injection. With these experiments, the instrument setup consists of a pump with two 10 mL syringes (generally filled with the same buffer as the injected specimen) that are responsible for the constant flow throughout the entire system with the flow rate set to 5  $\mu\text{L}$  per minute (to ensure and maximize the solution's interaction with the gold and/or SAMs on it) that are connected through extensive tubing to the flow cell of the system where the surface is located after mounting. The introduction of the sample solutions is done with a 500  $\mu\text{L}$  syringe through the injection valves that are either open (during injection) or closed (outside of the time of injection) at any given time to create continuity of the flow, into the injections loops of either 100 or 250  $\mu\text{L}$  volume size, and finally into the overall flow of the system. Most of the components listed can be seen in Figure 11. The flow system is open at the end, so, once the solution has gone through the flow cell, came into contact, and had sufficient time to interact with the mounted surface, it flows out of the system into a waste collection container. The data is collected on the connected PC throughout the entirety of the single day's experimental session.

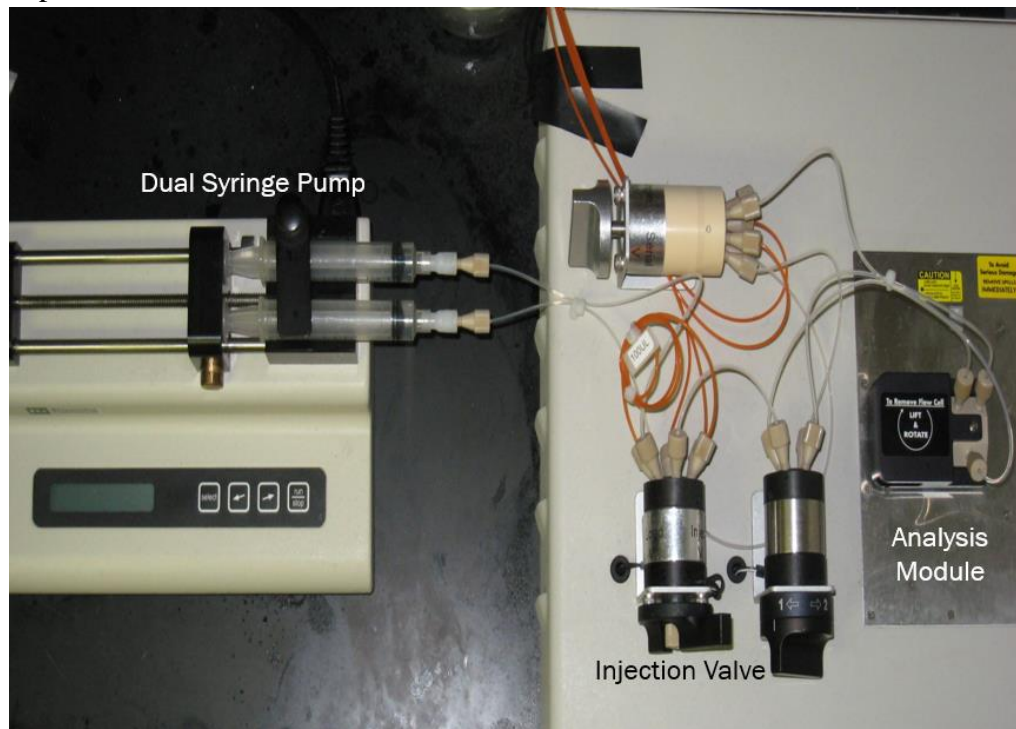


**Figure 11.** An image of the actual setup of the BI 2000 SPR system used in this research with labeled positions for the components of the instrument.



## Results and Discussion

### *Dendron-DNA Conjugate Synthesis*

All the reactions of this synthesis have been established in literature<sup>6,7</sup>, and all the materials utilized throughout the synthesis are readily, and commercially available. As it was indicated previously, the order of the reaction steps is crucial for the production of the conjugates. As indicated in Figure 3 (a), first, the functionalization of the primary amines on the periphery of the G4 dendrimer had to be completed. This reaction serves two purposes – it places a functional group that is going to be utilized for conjugates' attachment to the gold substrates and keeps it protected until required at the same time. The thioacetate groups are placed on the dendrimer periphery through a nucleophilic substitution reaction between the primary amines and the NHS-esters of the SATP molecules. After the first reaction, the solution is diafiltered at least twice to rid it of the extraneous SATP to prevent its potential future attachment to gold through the same interactions after SATP's deacetylation. After this, the single-point attachment sites for maleimide-activated ssDNA were provided by reacting the thioacetate-terminated dendrimers with TCEP in order to reduce the disulfide bond at the core of the dendrimer and produce thioacetate-terminated dendrons, each with a site for sSMCC-modified ssDNA conjugation (Figure 3 (b)).

Amine-terminated 5'-amine-modified 3'-biotin-modified ssDNA and 5'-amine-modified ssDNA without the biotin modification were both attached to the thioacetate-terminated dendrons with the help of the heterobifunctional cross-linker sSMCC mentioned previously as two separate syntheses with similar conjugates as products. The linking of sSMCC to ssDNA happened through a nucleophilic substitution reaction which resulted in the formation of a stable amide bond between the amine group modification of the ssDNA molecules and the NHS-ester of sSMCC (Figure 3 (c)). The resulting products of the reactions were diafiltered at least twice to remove extraneous

sSMCC to prevent any unwanted linking of sSMCC to other primary amines that were present on molecules utilized in this synthesis. The maleimide-activated ssDNA was then reacted with the thioacetate-terminated dendrons with the sulfhydryl group as a single-point site for the attachment with a 3-fold excess of the dendron products. This reaction formed a stable thioether bond between the dendrons and ssDNA molecules via a Michael addition reaction (Figure 3 (d)) after it was allowed to go to completion overnight to achieve a potentially higher yield.

As stated previously, the order of the reactions completed throughout this synthesis is quite crucial, as it is important to avoid the possible formation of any and all side products. One of the examples of such side products would occur if the primary amine groups on the dendrimer periphery were not functionalized first prior to their reaction with the maleimide-activated ssDNA. In conditions that either are or resemble physiological, the primary amine groups present on the periphery of the dendrons are positively charged while the phosphate backbone of ssDNA is polyanionic. This would present trouble because of the fact that all of the synthesis reactions are conducted in pH 7.2 PBS, which is relatively close to that of physiological conditions, and would result in a product of dendrons and ssDNA molecules that would aggregate due to their electrostatic interactions and precipitate out of solution.<sup>6, 7</sup> That is exactly why the functionalization of the primary amines present on the periphery of the dendron is done first, as it not only provides the desired functionality but also prevents this side reaction from occurring while allowing the reaction of interest between the maleimide-activated ssDNA to happen only at the site where it is required. In addition to this, the post-SATP functionalization thioacetate-terminated dendrimers are stable in aqueous solutions of the pH 7.2 PBS, which allows them to be stored for prolonged periods of time (couple of months), if required.

Additionally, reacting the terminal amines first and placing the thioacetate protection on the dendrimers' periphery is complete, the core disulfide bond of the dendrimers is cleaved by the addition of TCEP in excess in order to provide the free thiols. This ensures that there is now only one possible site for the maleimide-activated ssDNA to be attached to, which in turn creates a one-to-one ratio of the ssDNA strands to dendron (1:2 for the whole dendrimer molecule). The reaction of the amine-modified ssDNA is completed directly prior to the future addition of the maleimide-activated ssDNA to the cleaved thioacetate-protected dendrons. This is done because of the relatively short lifetime of the two reactive groups of the maleimide-activated ssDNA – the NHS-ester readily hydrolyzes at the physiological pH, having a lifetime of approximately 8 hours, while the maleimide can be stable for several hours.<sup>6, 7</sup> As discussed previously, both thioacetate-terminated dendrimers and maleimide-activated ssDNA must be purified prior to the thiol-maleimide reaction through the use of the Amicon Ultra centrifugal filter devices in order to remove any extra SATP and sSMCC. For sSMCC, it could react with any sulfhydryl-containing dendrons without the attachment of maleimide-activated ssDNA and form that side-product, whereas, for SATP, it could react with any primary amines present on the ssDNA strand, whether it is the desired reaction at the 5' modification site or any free primary amines present on the strand itself.

#### *Purification and Extraction of the Conjugates (Gel Electrophoresis)*

After the completion of the conjugate synthesis (aside from their deprotection with hydroxylamine), they had to be purified via gel electrophoresis procedure described in the corresponding Experimental section. This was done to remove excess dendrons that were left unreacted as well as any unmodified (by sSMCC) ssDNA that was not conjugated. The removal of these excess reactants is necessary to ensure that nothing interferes with the tethering of the

synthesized conjugates to the gold. As stated before, the phosphate backbone of the ssDNA can cause issues throughout the synthesis procedure, however, it can also interact with the gold, as it has a natural affinity and can physisorb to gold.<sup>6</sup> This presents a problem, as it would mean that the unreacted ssDNA would compete for binding sites with the conjugates, interfering with the overall functionality of the SAM as a whole. A similar problem arises from having excess dendrons present (3:1 dendron to DNA ratio), as upon the deacetylation reaction, the functionalized dendrons would bind to the gold also competing with the conjugates and preventing continuous monolayer formation of them, which is why they must be and are removed from solution over the course of the synthesis, purification, and extraction.

The purification of the ssDNA-dendron conjugates was done via using 4% agarose gels. As established in literature before, usually, short ssDNA sequences such as the ones utilized in this research (18 bases) are separated using polyacrylamide gels. It was found previously, however, that the utilization of polyacrylamide gels in order to separate the unreacted ssDNA was problematic as it caused difficulties with the removal of the small polyacrylamide particles from the recovered conjugates, which would, in turn, interfere with the continuous and uniform formation of the SAM on the gold surface.<sup>6, 7</sup> This is the biggest reason why the purification and extraction procedure utilized agarose gels instead, and they were made 4% to achieve required appropriate separation of small generation (G4) dendrimers, ssDNA-dendron conjugates, and the unreacted ssDNA.

As mentioned already, the extraction of the conjugates from the gels was done by physically cutting out the visible bands of the gel, where it is believed conjugates would be, as a piece of gel. As illustrated in Figure 12, a successful synthesis led to the observation of the hindered conjugates' bands in the gel (a) and (b), which were then excised to be imaged as

presented in (c). Lane 1 was used as a reference for the unreacted ssDNA to not be mistaken with the reacted conjugates and was loaded with a lower concentration of the same ssDNA strand utilized during synthesis, whereas lanes 4 through 8 were loaded with the actual products of the conjugate synthesis. Based on the previously established interactions of the contents of solution that contained conjugated product, unreacted ssDNA migrated through the gel towards the positively charged anode the furthest because of its innate negatively charged phosphate backbone and the absence of any hindering factors aside from the gel itself. The conjugated ssDNA-dendron complex molecules migrated at a slower rate due to the now higher mass of the molecules and were detected next. The unreacted dendrimers were not detected in the gels, as the dendrimer-specific stain was not utilized in this particular research and also, they are slightly positively charged and actually migrated towards the negatively charged cathode in the gel chamber and left the gel entirely.<sup>6</sup> All of these interactions of the solution contents that are loaded into the gel allow for an easy way to purify, detect, and excise the conjugates from the gel. Following the excision, the piece of the gel containing the conjugates is cut up and crushed into smaller pieces on a layer of parafilm and put into a falcon tube for the actual extraction from the gel with the 1x TAE buffer overnight. Although they are not as crisp, the bands for the ssDNA-dendron conjugates are evident as shown by the images in Figure 12. The presence and successful detection of this band was what verified the successful conjugation of the complex through the covalent bonds formed between the ssDNA and dendrons.

The reaction efficiency was determined by using the NanoDrop<sup>TM</sup> 1000 spectrophotometer instrument through determining the concentration of the nucleic acids present (ssDNA) before and after the purification and extraction via gel electrophoresis procedure described earlier. Examples of NanoDrop<sup>TM</sup> produced spectra could be seen in Figure 13. This was utilized because of the

ability of nucleotides to absorb UV light at specific wavelengths. Absorbance peaks at 260 nm (A260) and 280 nm (A280) are used by the instrument to quantitate the amount of DNA (dsDNA or, in this case, ssDNA) present in the measured aliquot (2  $\mu$ L) of the sample introduced to the instrument. The measurements are completed 3-5 times introducing a different aliquot of the same volume from the sample to ensure statistical significance of the resulting concentration value. Based on the average aliquot concentration obtained by the instrument, the concentration of the conjugate solution is calculated before and after the purification and extraction procedure to figure out the percent yield of the synthesis. Varying degrees of synthesis' success have been accomplished throughout the time of this research project, but the average yield of reaction was estimated to be between 20-35 percent each successful time.

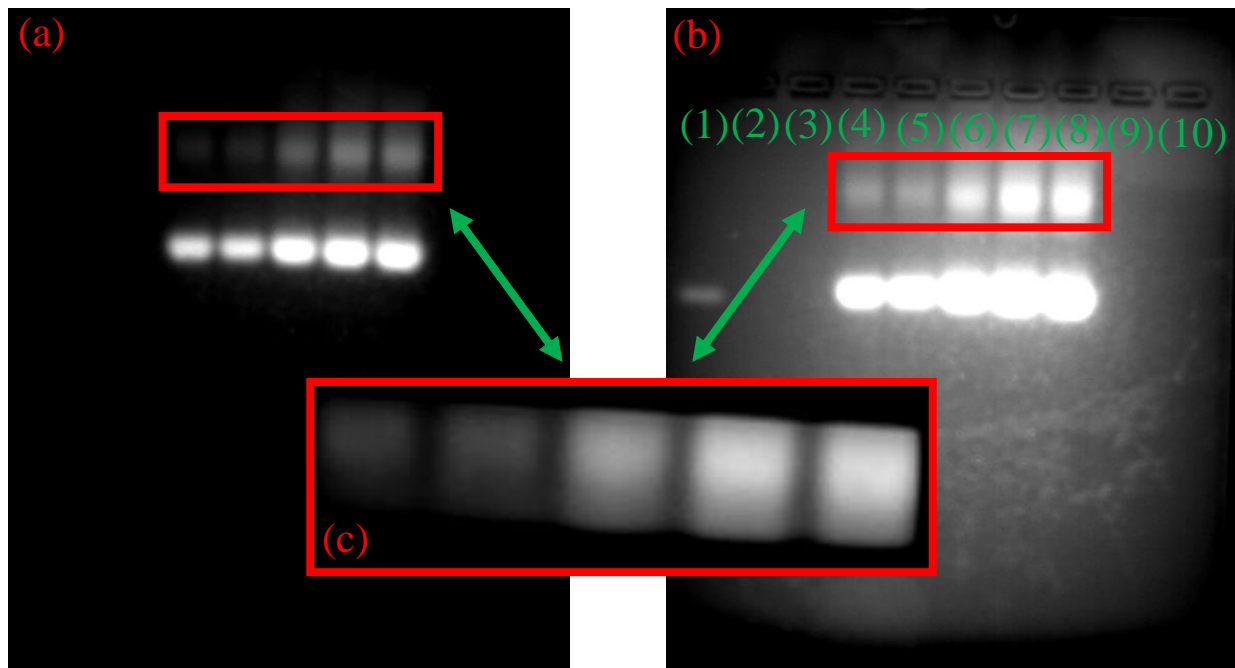


**Figure 12.** UV images of the EtBr-stained 4% agarose gels after gel electrophoresis of the G4 conjugates. This is done to extract the product from the unreacted starting materials and extraneous chemicals and purify them. The three UV images illustrated show the outcome of the same gel done for the G4 conjugate product purification and extraction. Images on the left (a) and right (b) differ only in their exposure level, while the one in the center (c) illustrates an actual gel piece cutout that was excised from the entire gel.

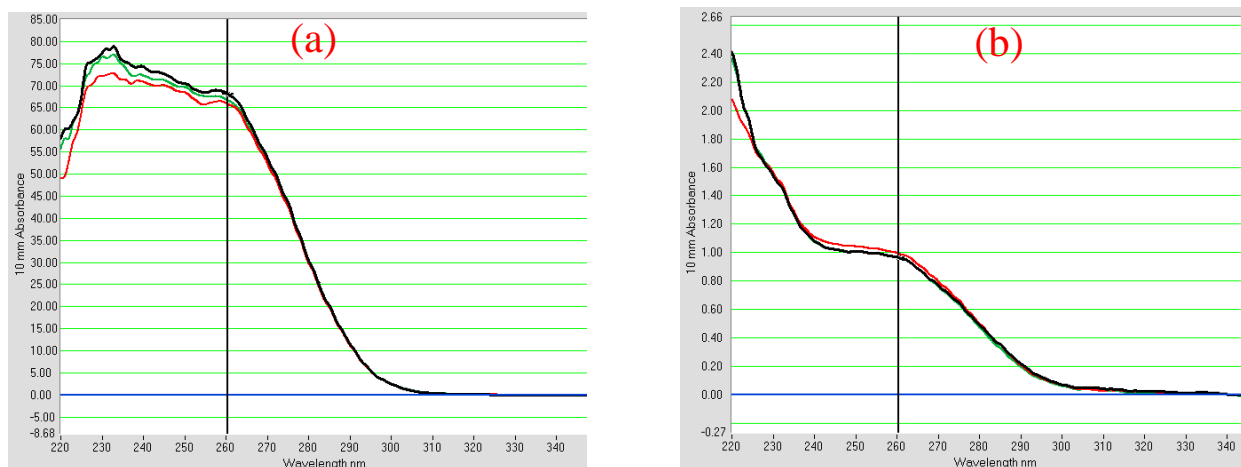


**Figure 13.** NanoDrop™ 1000 spectrophotometer plots of the nucleotide absorbance values at various wavelengths. The cursor at 260 nm is indicative of one of the peaks where the absorbance is observed for the present nucleotides of the aliquot loaded into the instrument. There are two total peaks that are used to quantitate the present ssDNA, but the peak at 280 nm more or less becomes part of the peak at 260 nm due to its higher absorbance value. In (a) values for the absorbance prior to purification and extraction procedure is shown, and in (b) values for the absorbance at the same peaks after the purification and extraction procedure is illustrated.

#### *Surface and Conjugate Preparation for Conjugate Attachment*

One of the factors that had to be taken into account when assembling a conjugate monolayer on gold was the cleanliness and readiness of the surface for the self-assembly. The procedure that was described earlier of the surface preparation for the conjugate attachment and assembly was followed for every single surface individually every time prior to self-assembly. That procedure made sure that, when attached, the monolayer was uniform everywhere throughout the surface of the gold, whether it was a pattern of HDT or MCH by itself, HDT or MCH with functionalized dendrimers, or HDT or MCH with conjugates. The combination of several cycles of sonication with isopropanol as well as plasma cleaning of the surface altogether ensured the surfaces were clean of any organic contaminants and prepared them for any subsequent direct exposure to the functional groups of the conjugates (thiols). The effectiveness of this designed preparational cleaning procedure was tested via two different techniques utilized throughout this

research – scanning electron microscopy and atomic force microscopy. Both techniques’ results led us to believe that the procedural protocol followed for cleaning the surfaces provided us with surfaces that had the appropriate cleanliness and mean roughness to be able to be used for self-assembly of the monolayers and their features’ detection. Research conducted later on during the span of its entirety, however, indicated that the procedure of cutting and cleaning the surfaces was slowly but certainly introducing physical abrasions and extraneous materials. This would result in either difficulty of completing the physical collection of height profile through utilization of AFM or the inability of analysis of said profiles due to the designed HDT or MCH pattern being unclear, interfered with by the presence of undesired materials, or absent altogether. The experiments that could be conducted were completed with the surfaces that provided for a good ground for the height profile collection and analysis, but ultimately it was decided to investigate this surprising issue further in the future. Examples of surfaces that were questionable are illustrated in Figure 14. Some of the examples of acceptable surfaces are shown in Figures 15 and 16.

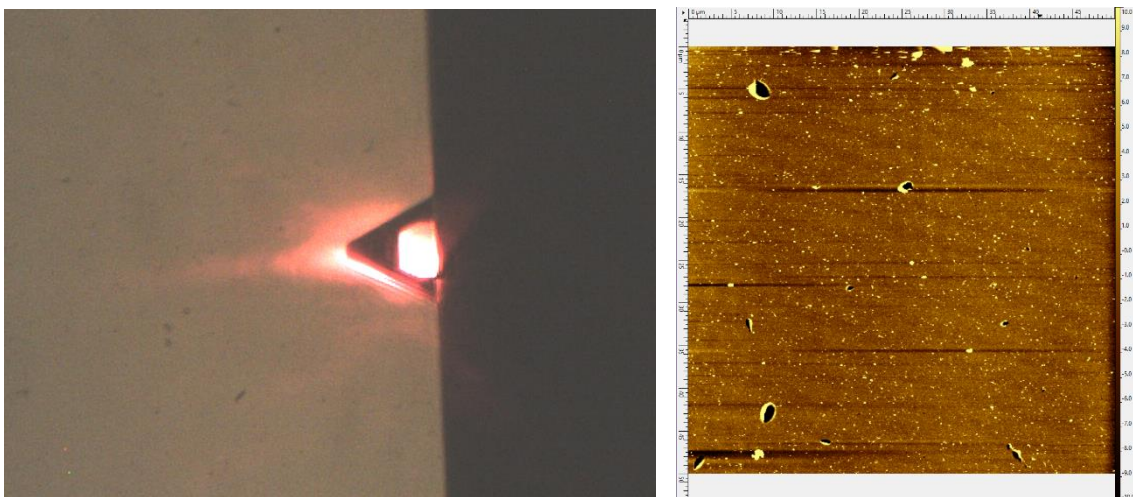


**Figure 14.** Camera and AFM images showing the physical abrasions and unwanted materials being present on a surface that had undergone the designed cleaning procedure described previously.



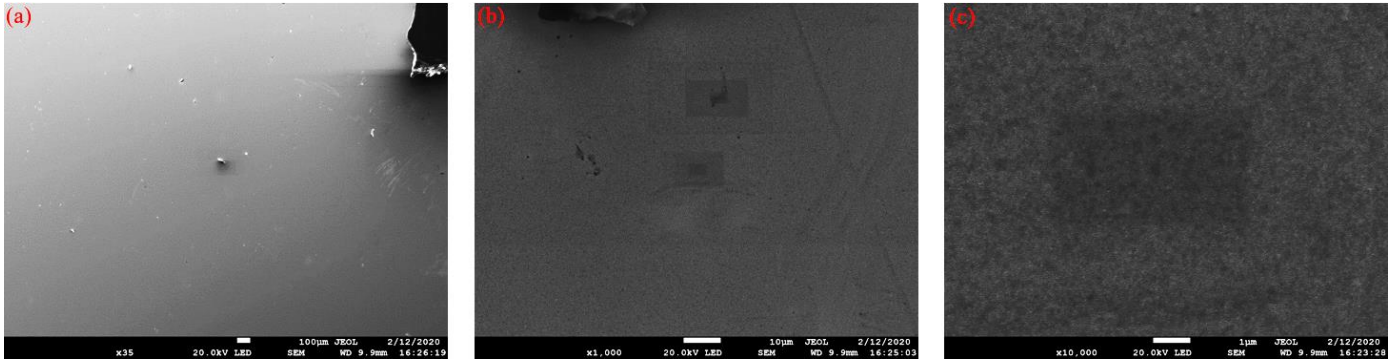


**Figure 15.** SEM images of the bare CA134 EMF evaporated Cr/Au surface after the cleaning procedure at 20kV acceleration voltage, probe current of 12, working distance of 10 mm, and the magnifications of 35 (a), 1000 (b), and 10000 (c) collected through the JEOL Scanning Microscope 7200FLV (JSM7200). These images show uniformity of gold throughout the surface except for the couple of physical features seen in the first image – conducting tape and a single physical abrasion. The slight discoloration of the surface in (b) and (c) is due to the conduction of several SEM scans completed on the single studied surface and saturation of the gold with the electrons from electron beam of the JSM7200.

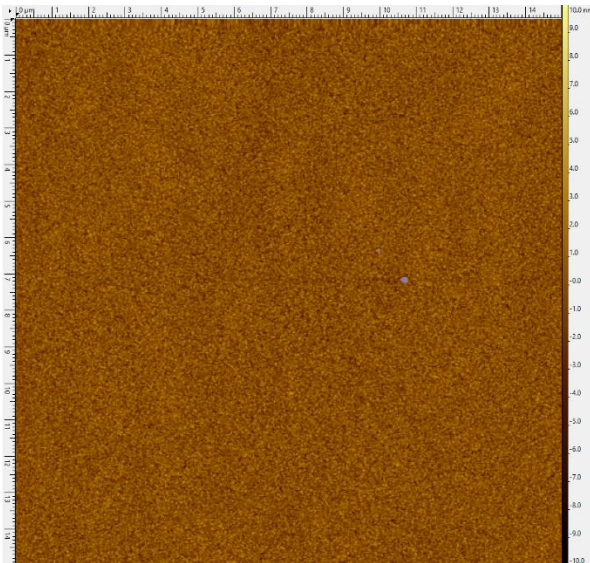


**Figure 16.** AFM image of the bare CA134 EMF evaporated Cr/Au surface (new) after the cleaning procedure collected through the MM8 SPM. The parameters for this scanned image were as follows: 50  $\mu\text{m}$  scan size, 0.75 Hz frequency of oscillation of the cantilever with the tip, and 1024 scans per line. The dot(s) appearing blue are masked regions that are either remnants of limited physical abrasion on the surface or imaging artifacts.

As this research progressed and the electric-potential-induced switching experiments began, most crucial part of this research had been addressed – switching of the SAM. As discussed prior, the designed SAM of choice was to be subjected to a reversible bias – electric potential – in order to observe the desired switching and varying conformations of the SAM. In this case, there had to be a way in which the potential would be applied directly to the surface and the change would be observed by conducting height profile collection experiments via AFM. Originally, it

was thought that soldering the wire directly to the gold surface would be the way of attachment and it was the only way of doing so successfully. However, with the increasing concerns for the introduction of extraneous physical abrasions or unwanted materials to the surface with this method, it was disregarded, and other ways had to be found. The first method that was attempted was to utilize conductive tape to secure the gold wire on the surface. For what it was worth, the tape worked in attaching the wire to the gold surface but unexplainably failed to provide conductivity between the wire and the gold while attempting to measure the resistance of the circuit with a voltmeter, as it indicated that there was no closed system and failed to give a value for its resistance. Next, conductive silver paint was tried, which would perform the same function in a different manner. With this silver paint, the application of it to the wire and gold surface proved, as it was proving challenging to get just the right amount of it and not have a considerably large object on the surface that would interfere with the AFM cell positioning and its' scanning capability. Once the setting/drying time of the paint was figured out, and it was on the surface with the wire attached, it was subjected to external pressure via directly pushing on the drop of it on top of the wire to spread it more and lessen the height of the drop. Ultimately, this worked fantastically for the attachment of the wire and the conductivity of the system, as was confirmed through the very same testing with a voltmeter. Once the first set of experiments with the AFM had been completed using the liquid cell, however, the wire and the whole drop of silver paint came off the gold surface after being exposed to the water utilized during the liquid scanning process of AFM. After this, it was ultimately decided to go with the EG 5810 silver epoxy adhesive as the facilitator of the wire attachment. There ended up being several benefits to using the silver epoxy: one, it was easy to prepare and use, as well as cure and attach to the surface, two, it provided the robust attachment of the wire to the surface, and lastly, its ability to provide continuous conductivity with

the surface was excellent, as indicated by the same tests conducted with the voltmeter. The system with the silver epoxy allowed for the completion of the experiments on height profile collection with the AFM. Nonetheless, it resulted in ultimately finding out that the robust attachment only lasted for so long and ended up following a close case of the silver paint from before. The drop of epoxy that was used would, most of the time, hold for the entirety of the series of AFM scans, but would buckle under the introduction of solution to the system. The wire tended to come off the surface, as it was the thinnest point of the attachment of the drop of epoxy on the surface, but the remaining epoxy would hold on to the surface. In that case, generally, another attempt was made to attach the wire via the use of the silver epoxy in another area of the studied gold surface, if the surface provided good height profiles during the image analysis. Another suspected problem of using the silver epoxy was that, during the setting and curing time, especially in the oven, the vapors of one of the components would migrate and find themselves on the gold as one of the extraneous materials that would later be detected by the AFM tip. One of the ways of mitigating this was attempted: the curing was done outside of the oven at room temperature for a period of 24 hours, as suggested by the manufacturer to be another way of curing the epoxy. This, however, resulted in similar outcomes both in terms of the robustness of the attached wire and the finding of nonessential materials on the gold surface.

During the procedure of cleaning, as it was mentioned before, the purified extracted conjugates are reacted with hydroxylamine to prepare them for future attachment to the gold. It was previously established<sup>6,7</sup> that this reaction's success can be monitored, and its rate of success can be obtained, too. A chemical reaction with excess 5,5'-dithio-bis-(2-nitrobenzoic acid) (Ellman's reagent) was completed in order to verify the deacetylation of the ssDNA/dendron complex due to the ability of the Ellman's reagent to react with free thiols and produce 2-nitro-5-

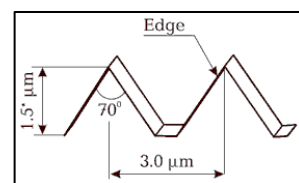
thiobenzoic acid, which produces a color change and absorbs at 412 nm. UV-Vis spectrophotometer can be used to assess the concentration of the 2-nitro-5-thiobenzoic acid present in the aliquot of the solution, but, in this research, it was qualitatively determined that the reaction had gone to completion by the appearance of a very obvious color change – transparent to dark yellow – and surmised that the deacetylation was successful. As supported by an earlier publication from this research group, the deacetylation reaction of the conjugates with hydroxylamine is high-yield ( $98 \pm 4 \%$ ) and goes to completion readily.<sup>6</sup>

#### *Polydimethylsiloxane (PDMS) Master Preparation and Microcontact Printing*

One of the aspects of this research that was chosen to be explored throughout some part of it was the arrangement of the conjugates on the surface in a way that would allow gathering of the height profiles in order to verify one of the requirements for the switchability – appropriate height of the SAM or length of the SAM's tail. Overall, the patterning of the SAMs on the surface is not required to achieve the desired quality of switchability of the SAM, however, one of the characteristics that can be assessed to support the hypothesis of the conjugates' ability to switch, eventually, is the length of the molecule's tail that will be responsible for the switching properties of the designed SAM. One technique that was used to measure and confirm this desired length was AFM and its measurements of height profiles of the SAM while present on the surface. In order to collect these height profiles correctly and accurately, the surface is patterned to provide a gradient and reference to be able to support the reliability of the resulting height profiles. This is accomplished by utilizing HDT or MCH and their natural ability to attach to gold through the thiol interacting with it. To be specific, HDT or MCH serve the purpose of the “ink” on the PDMS master that allows it to be arranged in a pattern during the exposure to the gold surface (see Figure 6 for a side view of the pattern). Once the gold surface has a pattern of HDT or MCH on it, it is

then backfilled with deacetylated conjugates to allow for their self-assembly in this patterned manner.

A couple of differing patterns produced from varying silicon wafers as PDMS masters were utilized in this research, however, ultimately, only one such master was chosen to be used consequently over and over again, as it produced the desired pattern that allowed for consistent patterning, its detection on the surface via AFM at desired settings, and successful analysis of the height profiles. Through experiments with techniques such as SEM, patterning itself, and AFM, the PDMS master produced from TGG1 silicon wafer was chosen to be the one utilized for patterning of HDT or MCH as per the described procedure. SEM and AFM experiments were completed on the wafers in order to confirm the lateral distribution of the physical patterns shown in Figure 17 that would result in the pattern on the PDMS master that is an inverse relief of the wafer's pattern, and after



selecting the appropriate pitch of the physical pattern, the corresponding wafer was selected to be used to make the PDMS master to be used subsequently throughout this research. Figure 18 demonstrates two resulting tested PDMS masters, one of which was the chosen master for further microcontact printing.

**Figure 17.** The pitch of the TGG1 (manufacturer's identifying number for the AFM grating) pattern on the silicon wafer.

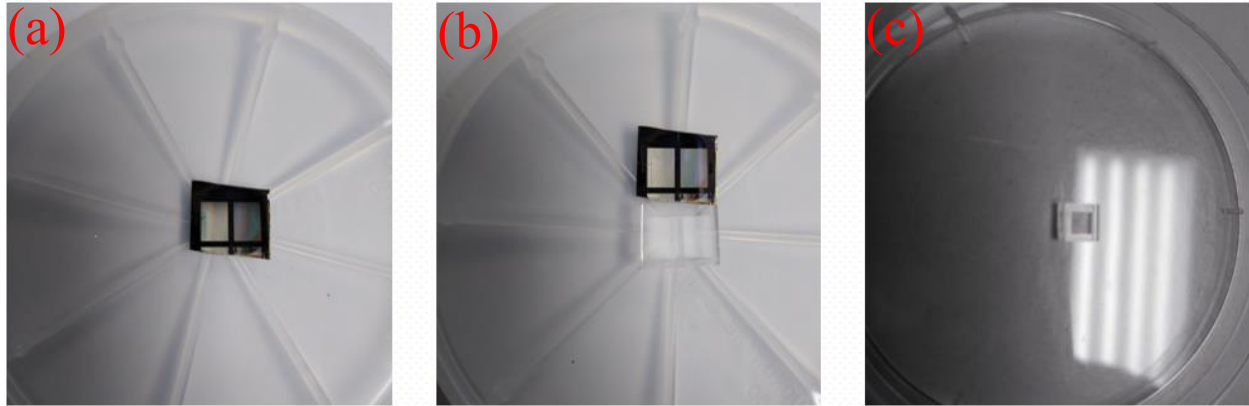


**Figure 18.** Optical images of (a) a piece of silicon wafer with the pattern of interest on it. (b) the same piece of silicon wafer sitting next to the PDMS master produced from it following the procedure described previously. (c) The PDMS master that has been used all throughout this research that was produced from the TGG1 grating on the silicon wafer also in accordance with the aforementioned procedure for PDMS master preparation.

#### *Atomic Force Microscopy (AFM) Experiments*

The first set of experiments completed during utilizing AFM was focused on measuring the roughness of the gold surfaces that were set to be used for microcontact printing of HDT or MCH and backfilling of the conjugates. Both old (>10-years-old) and new CA134 EMF evaporated Cr/Au surfaces were investigated using AFM to figure out if they had appropriate roughness (irregularities of the substrate surface) for us to be able to detect the height profiles of both the HDT or MCH and the conjugates accurately and correctly. After the successful completion of the previously discussed surface cleaning procedure, both were subjected to AFM scans in air with the parameters described previously. The analysis was done using the Gwyddion software and its built-in masking and automatic roughness calculation capabilities. From this set of experiments, it was deemed that the older gold surfaces, which had a mean roughness of varying degrees that ranged from 2.10 to 3.00 nm, was not to be used for future microcontact printing with HDT or MCH and self-assembly of the conjugates experiments, as the natural roughness of the surfaces themselves at this point would not allow for precise and accurate height profile measurements. Prior to ordering new surfaces and testing their roughness, there was an attempt to

mitigate this roughness of the old surfaces by annealing the gold surface overnight in an appropriate instrument. After post-annealing AFM scans, it was determined that the mean roughness value did diminish for some areas on the gold surfaces, but still fell into the range mentioned above (2-3 nm). After this particular experiment, it was established that using the old surfaces was not appropriate for the height profile measurements, and new CA134 EMF evaporated Cr/Au surfaces were acquired and scanned with AFM. The resulting mean roughness values of the new surfaces (Figure 16) were also obtained using Gwyddion and ranged from 1.03 to 1.10 nm. This value, although still relatively high (in comparison to the expected height of the HDT (2 nm)<sup>8</sup> or MCH (0.8 nm)<sup>11</sup>), was agreed to be more appropriate than the previous surface's values, so the new gold surfaces were used in the following experiments that involved microcontact printing, self-assembly, and height profile collection via AFM.

The next set of experiments involved using the newly acquired and tested EMF gold surfaces for the collection of the actual height profiles of self-assembled monolayers in both air and liquid environments with the help of microcontact-printed HDT or MCH on gold. The first scanned surface for this experimental set was one with microcontact-printed HDT and backfilled self-assembled deacetylated SATP-functionalized G4 dendrimer, shown in Figure 19 (a). The height profiles for the present backfilled functionalized G4 dendrimer were averaged out to be 3.75 nm as collected and calculated with the help of Gwyddion analysis software. This calculation involved using the value provided from the average heights obtained from Gwyddion and using the known height of the patterned HDT, which was approximately 2 nm, as reported in literature.<sup>8</sup> Adding these values provided the resulting value of  $3.93 \pm 0.09$  nm (95% confidence) for the thiol-terminated G4 dendrimers matched the unmodified G4 values previously reported values of 3.5-4.0 nm.<sup>12</sup>

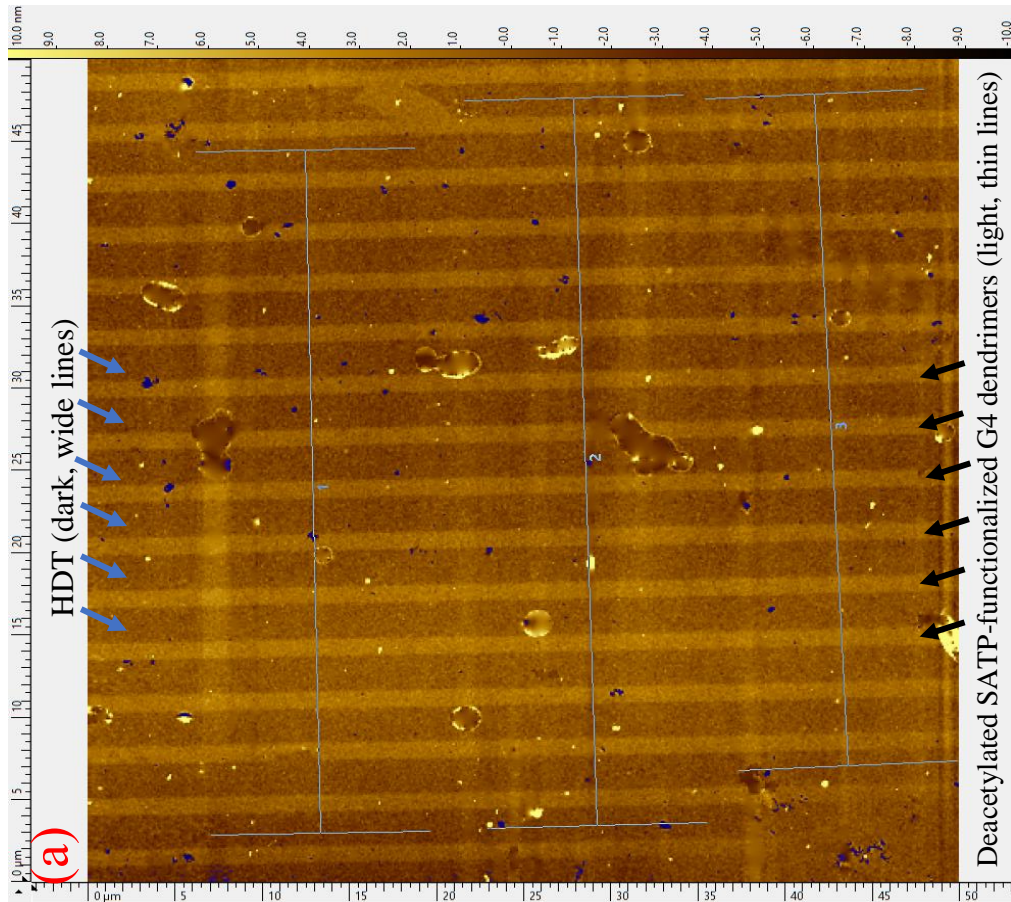
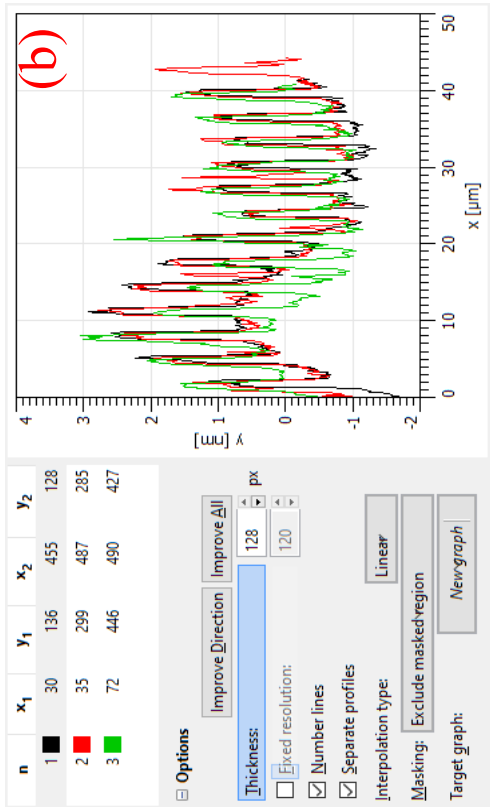


**Figure 19.** An AFM image of the gold surface that had been microcontact-printed with HDT and backfilled with deacetylated SATP-functionalized G4 dendrimers (white lines) in (a). The individual grains are either removed by performing Laplace interpolation (blurry) or masking them (dark blue) in Gwyddion software. In (b), these are extracted height profiles that reflect data under the highlighted three lines in (a) visible on the gold surface. Gwyddion averages the values under lines and provides a convenient output that can be analyzed further on a peak-by-peak basis.



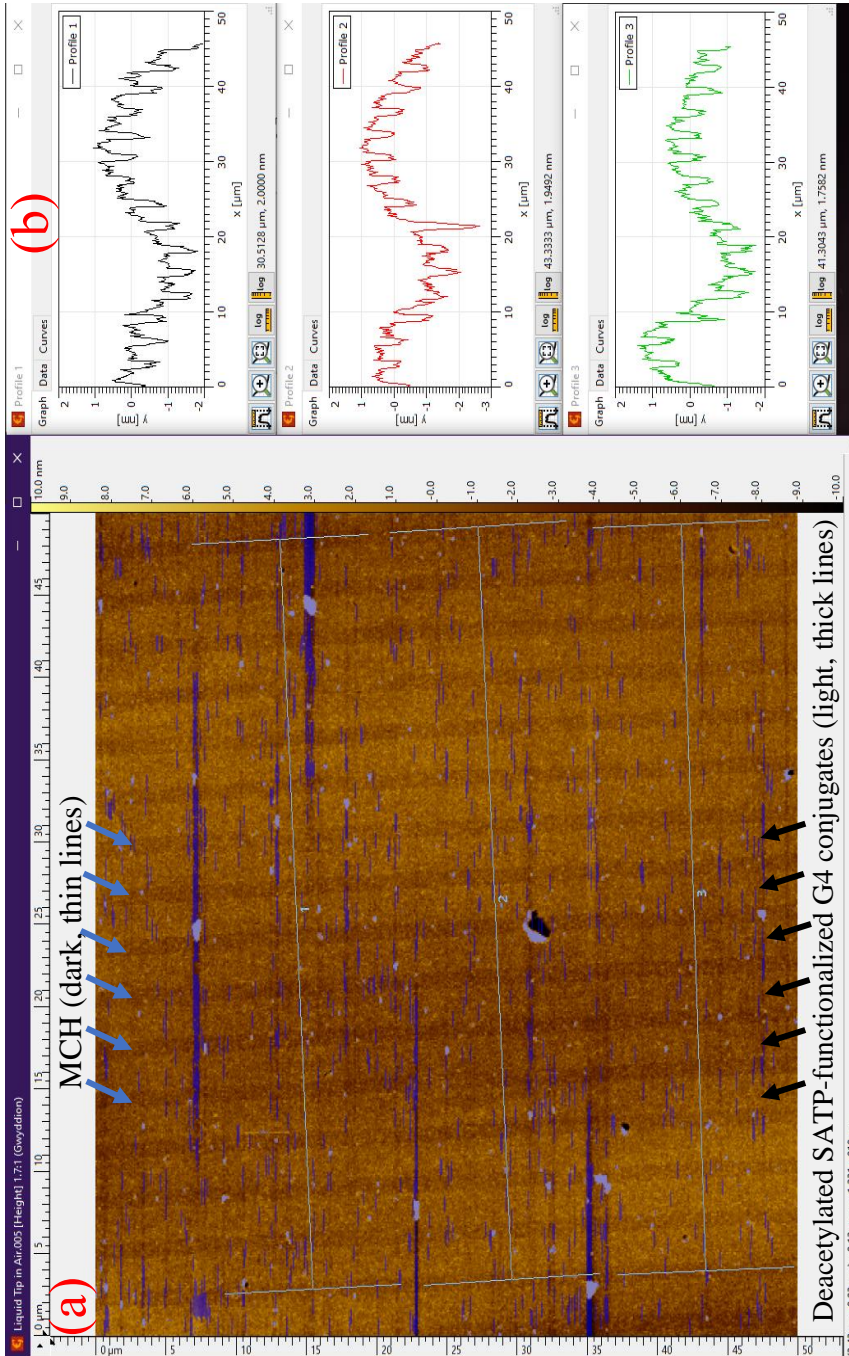


**Figure 20.** An AFM image of the gold surface that had been microcontact-printed with MCH and backfilled with deacetylated G4 conjugates (white lines) in (a). The individual grains and scars are masked (dark blue) in Gwyddion software. In (b), these are extracted height profiles that reflect data under the highlighted three lines in (a) visible on the gold surface.

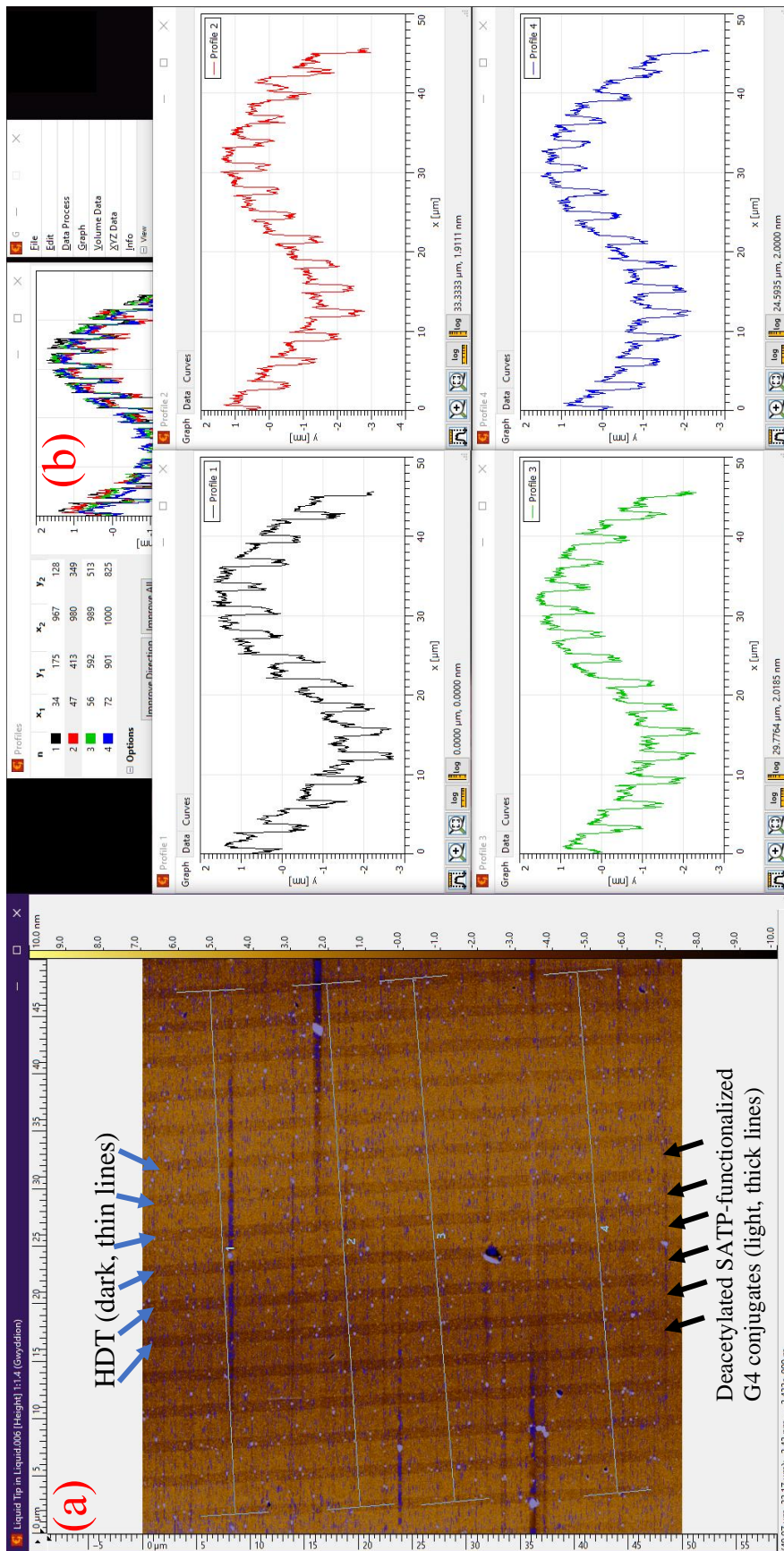


**Figure 21.** An AFM image from a liquid scan of the gold surface that had been microcontact-printed with MCH and backfilled with the designed SAM (white lines) in (a). The individual grains and scars are masked (dark blue) in Gwyddion software. In (b), these are extracted height profiles that reflect data under the highlighted four lines in (a) visible on the gold surface.

Following the completion of collection of the first set of heights, surfaces were prepared with actual conjugates following the designed assembly procedure as described previously. The latest change that was eventually implemented was the use of MCH instead of HDT during microcontact printing as the PDMS “ink” to provide a background pattern to the SAM. The MCH height value was found in literature to be 0.8 nm tall while on gold.<sup>11</sup> This change was done to see if, one, changing the pattern could result in mitigation or elimination of some of the extraneous features present on the surface at the time of imaging, however it was inconclusive whether it accomplished that particular goal due to little experimentation and time constraints towards the end of this research. The second reason was to produce a much larger gradient difference in heights between the background and the designed SAM while on the surface. The resulting processed image example can be seen in Figure 20. The heights obtained for the presumed conjugate “steps” with MCH as the background (0.8 nm included in the height value) and scanning in air ended up averaging out to  $1.66 \pm 0.04$  nm tall (95% confidence) after the calculation.

After the air scanning was complete, the water was pumped into the system with the same surface using the liquid cell’s tubing. Following that, the set of experiments that involved scanning in liquid was completed in the same manner with the previously described AFM preset and procedure. This scanning in liquid was completed on the same area as the air scan. One of the resulting processed images can be observed in Figure 21. The averaged heights for presumed conjugate “steps” (already including the MCH height (0.8 nm) in the conjugates’ height value) obtained from the liquid media AFM scanning experiments were calculated to be  $2.07 \pm 0.04$  nm tall (95% confidence). These were expected to be higher due to the exposure to liquid both because of the dendron and the ssDNA conforming to the now present liquid (water).

Overall, from what was able to be accomplished, the AFM scanning results were deemed satisfactory and supported by literature to the available extent. The most important aspect of this research to be tested was switchability of the SAM on gold. As discussed in detail previously, the attachment of the wire and application of electric potential was required to be used as the reversible bias to induce the proposed conformational change between two different states of the SAM. The design for the system to be used was completed and several attempts were made to utilize it and observe the described change. Nonetheless, every method used to secure the wire and create a closed system for the future observations of switching had been unsatisfactory due to the eventual detachment of the gold wire from the surface under the stress of either physical handling while conducting experiments with it, or exposure to liquid media (which included conjugate solution during self-assembly). Due to this, the electric-potential-induced switchability experiments were postponed until a much more successful method of wire attachment and securing was discovered and tested to provide acceptable results.

#### *Surface Plasmon Resonance (SPR) Experiments*

The SPR experiments provided a lot of conclusive results for this research. As mentioned before, some of the data that could be acquired through the use of this analytical technique involved verification of self-assembly on the gold surface, calculating packing density of the G4 based SAM while assembled on the surface, and confirming the ability to capture biomolecule(s) of interest – streptavidin.

As shown in Figure 22, a multitude of injections are possible to include in a single day's set of experiments, and all can be analyzed properly with the Data Analysis software that comes with the SPR instrument. After the preparational procedures for the BI gold surface are complete, and the surface is mounted onto the prism with the matching fluid, the instrument is turned on and

run for ~ 10 minutes in order to establish a constant baseline that will be used for analysis of injections. The first two injections in Figure 22 illustrate successful attachment of the G4 conjugates (synthesized with non-biotinylated ssDNA) as can be easily seen from the angular shift and permanent change of baseline appearing in both injections. Multiple injections of the analytes (both deacetylated conjugates and others) are required and are usually performed to ensure that the surface is fully populated or that the molecules already assembled on the surface are capturing as many flown analyte ligands as possible. This approach also helps in figuring out the packing densities when desired, as in order to state that the surface is fully populated the change in baseline has to be either non-existent or negligible in comparison to the naturally occurring baseline drift throughout the experiment's run. The next two injections consisted of introducing complementary DNA with a biotin modification on the 5' end. In the end, what is desired for the designed switchable monolayers is to be able to act as a biomolecular detector for the analyte of choice (streptavidin, in this case). The interactions of biotin-streptavidin proteins are well-studied, as it was indicated previously and were chosen to be observed in this setting as the easiest and most accounted for in terms of biomolecular detection. That is why the strand of 5'-biotin-modified complementary ssDNA is introduced to provide the SAM with potential biodetecting capabilities of streptavidin. Although it may be not fully clear in Figure 22, there was an angular shift and a change in baseline post-biotinylated ssDNA injection each of the two times (See Appendix B for a more detailed analysis of the shifts). The value shown in this particular figure is not the best representing one, which would be  $184 \pm 17$  mDeg on average (95% confidence), as supported by multiple experiments performed by another student in this lab, however it is one that supported the hypothesis, nonetheless. This already pre-supported that the SAM is capable of biomolecular detection of ssDNA of choice that was complementary to the one used for synthesis of the

conjugates, but it was investigated further by injecting streptavidin into the system shortly after with the next two completed injections. As can be seen in Figure 22, once again, there was an angular and a baseline shift corresponding to the time of each injection of streptavidin, which supported the capturing capability of the biotinylated-ssDNA-hybridized SAM. With this, it was concluded for the first time that the designed conjugates were potentially capable of biodetection of any molecules of choice with proper considerations and specific design of the SAM. The last injection that was completed in the same experiment was an injection of NaOH to hydrolyze the dsDNA and “reset” the SAM to the original state of post-self-assembly. This part of the experiment served a purpose of showing the reproducibility and repeatability of the experiment, as every step starting with the injection of biotinylated ssDNA was successfully completed once more and produced similar results of angular and baseline shifts. This was, of course, an indication of continuous capability of biomolecular capture by the designed SAM based on the previously established system of interaction between biotin and streptavidin. The next step of confirming the capability of the SAM to be able to capture a molecule of interest was involved using a ssDNA modified with biotin on its 3' end during the conjugate synthesis and use those conjugates for self-assembly on the gold and biodetection experiments.

In addition to confirming biodetection capabilities, one of the other aspects previously mentioned was determined using the SPR analysis – the packing density of the G4 SAM while on the surface. From the obtained and analyzed data, the angular shifts of baselines can be measured and used for this exact purpose. Within the SPR instrument's manual there can be found the following relationships between the angular shift and resonance units (RU) as well as between RUs and mass per square millimeter. From this, a conversion of the angular shift signal from the

SAM (435±60 RU average (95% confidence) for a populated surface) to the actual physical value of either molecules per unit of area or vice versa can be made in the following way:

$$0.73 \text{ RU} = 7.3 \times 10^{-5} \text{ Deg} \quad \text{and} \quad 1 \text{ RU} = \frac{10^{-12} \text{ g}}{1 \text{ mm}^2}$$

$$0.435 \text{ Deg} \times \frac{0.73 \text{ RU}}{7.3 \times 10^{-5} \text{ Deg}} \times \frac{10^{-12} \text{ g}}{1 \text{ RU} \times \text{mm}^2} \times \frac{100 \text{ mm}^2}{1 \text{ cm}^2} = 4.35 \times 10^{-7} \frac{\text{g}}{\text{cm}^2}$$

$$4.35 \times 10^{-7} \frac{\text{g}}{\text{cm}^2} \times \frac{1 \text{ mol}}{15,896.313 \text{ g}} \times \frac{6.022 \times 10^{23} \text{ molecules}}{1 \text{ mol}}$$

$$= \mathbf{1.65 \pm 0.25 \times 10^{13} \frac{\text{molecules}}{\text{cm}^2}}$$

$$\text{or} \quad \frac{1}{1.65 \times 10^{13} \frac{\text{molecules}}{\text{cm}^2}} = \mathbf{6.05 \times 10^{-14} \frac{\text{cm}^2}{\text{molecule}}}$$

This calculated density value ((1.65 ± 0.25) × 10<sup>13</sup> (95% confidence)) for the SAM designed with G4 dendrimers is just outside the range of switchability (10<sup>12</sup>-10<sup>13</sup> molecules per cm<sup>2</sup>) as indicated by Rant et al. in their research on SAM switchability using fluorescence as a confirmational analytical technique for the switching experiments.<sup>13</sup>

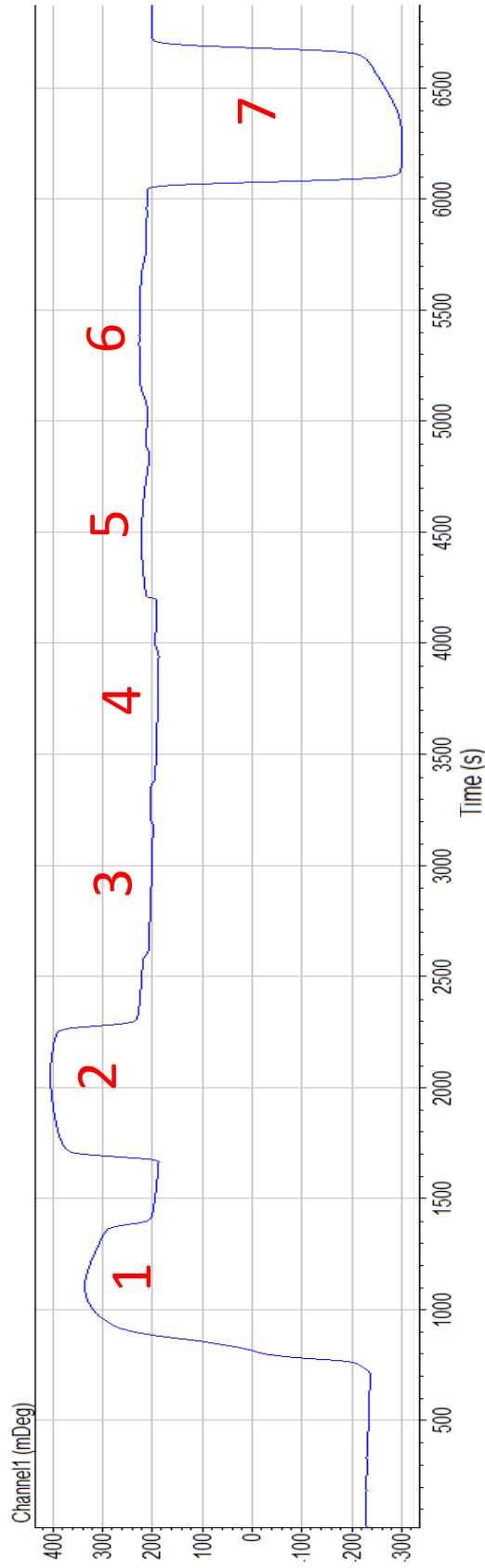


**Figure 22.** An example image of a day's worth of SPR experiments. Multiple injections are illustrated and labeled accordingly. The first two injections were G4 conjugate injections. Injections 3 and 4 included introducing 10  $\mu$ M Biotinylated Complementary DNA to the SAM on the gold. Injections 5 and 6 consisted of adding 10  $\mu$ M Streptavidin each time to the SAM with the complementary biotinylated DNA attached for the biomolecule detection testing. Lastly, injection 7 was 5 mM NaOH to disassemble the DNA double helix and leave just the SAM on the surface. This last injection is done so that the system can be used again for the same injections of biotinylated DNA followed by streptavidin to support reproducibility of biomolecular detection capabilities of the designed G4 SAM. The zoomed in and broken-down version of each peak can be found in Appendix B: SPR Multi-Injection peak analysis.



## Summary

This study describes successful synthesis of and investigation into the conjugates of generation 4 dendrimers and varying maleimide-activated ssDNA 18-mers for potential switchable biodetector capabilities. Dendrimer functionalization (and deacetylation) and cleaving were confirmed by utilizing the Ellman's reagent and its reaction with free thiols. G4 dendron conjugation to maleimide-activated ssDNA of choice was confirmed by gel electrophoresis experiments. Successful extraction and acceptable yields were accomplished by excision of conjugate bands from the completed gel electrophoresis experiments gels and NanoDrop UV-Vis ssDNA concentration measurements prior to and post-purification and extraction.

In addition, this study also shows the achieved assembly of the designed G4 SAM while on a patterned surface. As discussed in detail previously, the EMF gold surfaces were patterned using microcontact printing and characterized using AFM, and switchability experiments were attempted. A couple of G4-derived products were investigated, which included simple SATP-functionalized dendrimers and G4 conjugates with maleimide-activated unmodified ssDNA. The resulting AFM images and analysis indicate literature-supported values for the heights of the previously reported and analyzed molecules (functionalized dendrimers),<sup>12</sup> as well as some newly discovered and reasonably within expectations resulting values for the various conjugates. There were attempts to conduct the switchability experiments to observe the potential capability of the designed G4 SAMs to change between conformations, however, those studies were curtailed due to the difficulties encountered during the process of collecting AFM images in liquid medium due to the surface-bound wire coming loose during (or prior to) multiple attempts for data collection.

Lastly, the biosensing ability of the designed conjugates was confirmed partially by conducting SPR experimentation. These SPR experiments described previously focused on utilizing the same conjugates from the synthesis that used non-biotinylated ssDNA strand to detect

both its complementary strand of ssDNA with a biotin modification attached and the example analyte streptavidin. As per the resulting data, the designed G4 SAMs were indeed capable of functioning as a biodetector to capture the molecules of interest introduced in the SPR instrument following the self-assembly of the conjugates on the BI gold surfaces. The repeatability and reproducibility of the resulting conclusions about biosensing properties of the SAMs were tested throughout this portion of the study and were concluded to also be accomplished.

### **Future Work**

Some of the future work includes following similar procedures described throughout this entire research but expanding it further by utilizing various generations of dendrimers, as they may prove more promising in some respects than used G4 dendrimers. The varying sizes of the multiple different generations of dendrimer would be directly influencing such aspects of this research as synthesis yields, success of purifications/extractions, packing density while on surface, and switchability directly. Another manipulation that could affect similar areas of this research would be choosing different lengths of ssDNA strands used during synthesis. This, as supported previously, could also provide potential differing outcomes which would be of interest to further investigation.

The most important aspect that was not concluded during this research and needs to be investigated further is the switchability potential of these designed conjugates overall. Due to some unforeseen circumstances with the electric-potential-induced switchability testing experiments, it was eventually pushed into the category of work to be completed in further studies. The main aspect to be addressed, which may be the solution this research needed, is a way of attaching the wire to the gold surfaces in a much more efficient and successful way. Following this, the switchability experiments utilizing AFM should provide no further difficulties. Lastly, for the

AFM experimentation, conjugates with the biotinylated ssDNA and their height profiles need to be collected. With these conjugates, besides their height assessment, the switchability will be tested directly on the AFM in addition to testing it with the completed biosensing SPR experiments.

Lastly, one of the experimental designs to also confirm switchability mentioned briefly is the conduction of fluorescence microscopy experiments. The idea and design for these experiments came from an article by Rant et al.: the conjugates design would remain unchanged save for one addition – a fluorescent tag on the conjugated ssDNA that is going to be used as an indicator of the switching capabilities of the designed SAM.<sup>13</sup> These experiments would utilize a similar principle of using electric potential as a reversible bias applied to the gold with the SAM. In this case, the indicator of switching would still be a conformational change, but it would be detected not by a change in the observed height of the monolayer while subject to varying applied potentials, but rather by observing the presence or absence of fluorescence of the tag. This technique relies on a special gold atoms' property to quench the fluorescence while the source of fluorescence is close to it and not affecting it while it is away.<sup>13</sup> This would support the hypothesis of the switchability of the designed SAM even further and provide greatly reliable data in supplement to the future switching data from AFM experiments.

## References

1. Mehrotra P. Biosensors and their applications - A review. *J Oral Biol Craniofac Res.* **2016**, *6* (2), 153-159
2. Biosensors Market by Type, Product (Wearable, Non-wearable), Technology, Application (POC, Home Diagnostics, Research Lab, Environmental Monitoring, Food & Beverages, Biodefense) and Region (2021-2026)  
<https://www.marketsandmarkets.com/Market-Reports/biosensors-market-798.html>,  
2021
3. Love, J. C.; Estroff, L. A.; Kriebel, J. K.; Nuzzo, R. G.; Whitesides, G. M., Self-Assembled Monolayers of Thiolates on Metals as a Form of Nanotechnology. *Chemical Reviews* **2005**, *105* (4), 1103-1169.
4. Ulman, A., Formation and Structure of Self-Assembled Monolayers. *Chemical Reviews* **1996**, *96*, 1533-1554.
5. Lahann, J. S. M., Tran, T. N., Kaido, H., Sundaram, J., Choi, I. S., Hoffer, S., Somorjai, G. A., and Langer, R. A Reversibly Switching Surface. *Science* **2003**, *229*, 371-374.
6. B. Scott Day, Larry R. Fiegand, Erik S. Vint, Wanqiu Shen, John R. Morris, and Michael L. Norton. Thiolated Dendrimers as Multi-Point Binding Headgroups for DNA Immobilization on Gold. *Langmuir* **2011**, *27* (20), 12434-12442
7. Christian N. Warner, Zachary D. Hunter, Destiny D. Carte, Tyler J. Skidmore, Erik S. Vint, and B. Scott Day. Structure and Function Analysis of DNA Monolayers Created from Self-Assembling DNA–Dendron Conjugates. *Langmuir* **2020**, *36* (19), 5428-5434
8. Kumar, A., Biebuyck, H. A., and Whitesides, G. M. Patterning Self -Assembled Monolayers: Applications in Materials Science. *Langmuir* **1994**, *10*, 1498-1511

9. Xia, Y. and Whitesides, G. M. Extending Microcontact Printing as a Microlithographic Technique. *Langmuir* **1997**, *13*, 2059-2067
10. (2009). BI-2000 SPR system user's manual. Tempe, AZ: Biosensing Instrument Inc.
11. Takumi Hiasa, Hiroshi Onishi. Mercaptohexanol assembled on gold: FM-AFM imaging in water. *Colloids and Surfaces A: Physicochemical and Engineering Aspects* **2014**, *441*, 149-154
12. Andreas Hierlemann, Joseph K. Campbell, Lane A. Baker, Richard M. Crooks, and Antonio J. Ricco. Structural Distortion of Dendrimers on Gold Surfaces: A Tapping Mode AFM Investigation. *Journal of the American Chemical Society* **1998**, *120* (21), 5323-5324
13. Rant, U., Arinaga, K., Fujita, S., Yokoyama, N., Abstreiter, G., and Tornow, M., Dynamic Electrical Switching of DNA Layers on a Metal Surface. *Nano Letters* **2004**, *4* (12), 2441-2445

## Appendix A: Approval Letter



Office of Research Integrity

February 17, 2022

Eduard Lukhmanov  
1040 20<sup>th</sup> Street, Apt. 2  
Huntington, WV 25703

Dear Eduard:

This letter is in response to the submitted thesis abstract entitled "*Spatially Controlled Monolayers for Electrically Switchable Biomolecule Detection*." After assessing the abstract, it has been deemed not to be human subject research and therefore exempt from oversight of the Marshall University Institutional Review Board (IRB). The Code of Federal Regulations (45CFR46) has set forth the criteria utilized in making this determination. Since the information in this study does not involve human subjects as defined in the above referenced instruction, it is not considered human subject research. If there are any changes to the abstract you provided then you would need to resubmit that information to the Office of Research Integrity for review and a determination.

I appreciate your willingness to submit the abstract for determination. Please feel free to contact the Office of Research Integrity if you have any questions regarding future protocols that may require IRB review.

Sincerely,

Bruce F. Day, ThD, CIP  
Director

**WE ARE...MARSHALL.**

One John Marshall Drive • Huntington, West Virginia 25755 • Tel 304/696-4303  
A State University of West Virginia • An Affirmative Action/Equal Opportunity Employer

## Appendix B: SPR Multi-Injection Peak Analysis

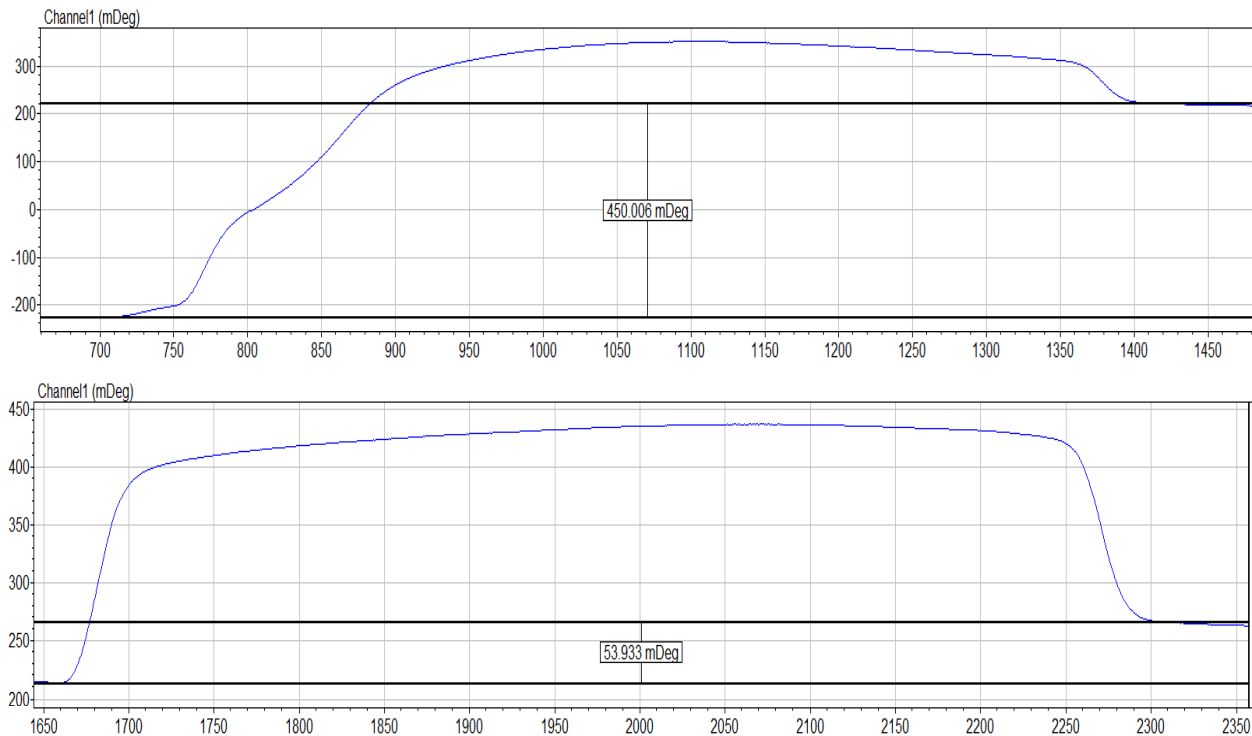


**Figure B1.** Images showing the two G4 conjugate injections at 605 and 1515 seconds zoomed in to show detail of the angular shift. These are shown in the analysis mode, where it can actually be determined directly from the instrument-produced data how much angular shift

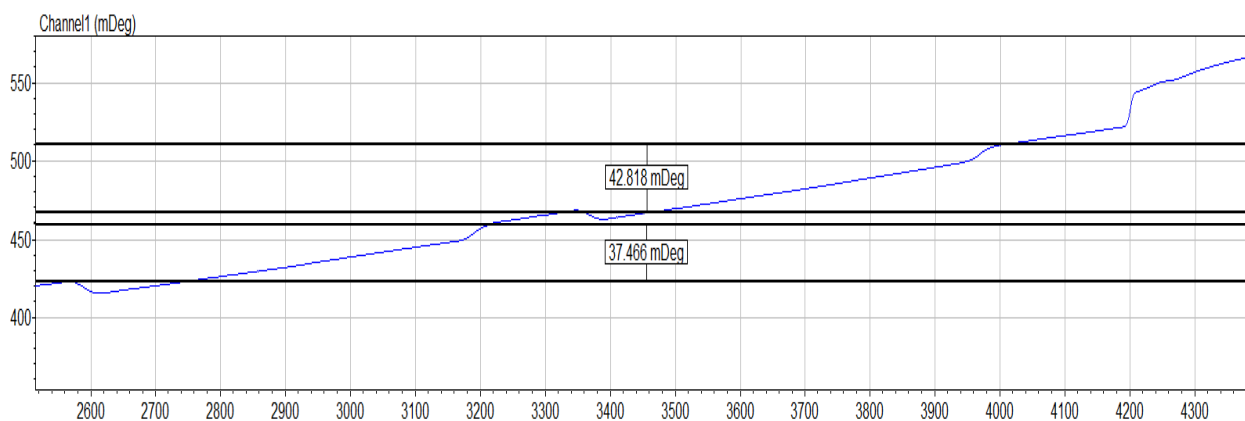


**Figure B2.** An image showing the two injections of 10  $\mu$ M biotinylated complementary DNA at 2425 and 3205 seconds zoomed in to show detail. The highlighted illustrated angular shifts allow for the verification of successful DNA hybridization.

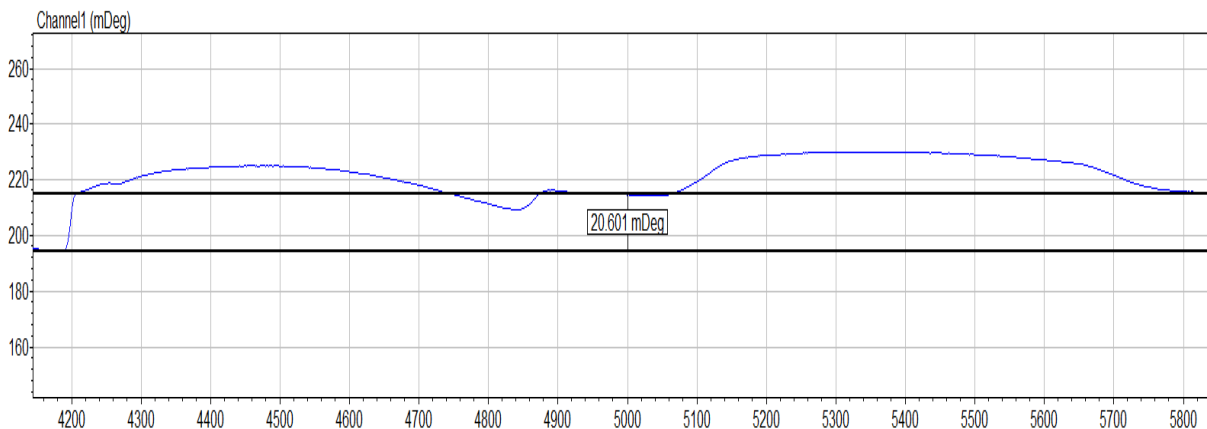


**Figure B3.** An image showing the two injections of 10  $\mu\text{M}$  streptavidin at 4100 and 4960 seconds zoomed in to show detail. The highlighted illustrated angular shifts allow for the verification of successful biomolecular capture of streptavidin by the biotin present on the SAM through the hybridized biotinylated complementary DNA.

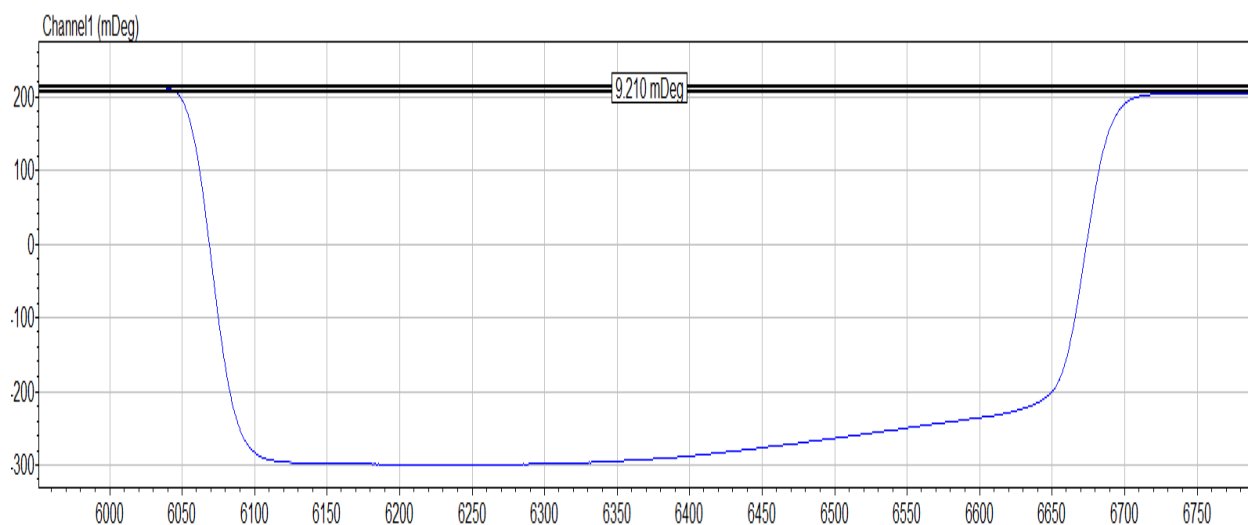


**Figure B4.** An image showing the last injection that consisted of 5 mM NaOH. Once again, this injection was done in order to hydrolyze the now double stranded DNA complex with captured streptavidin to reset the SAM system on the gold surface and reproduce the experimental results by conducting another set of injections in a similar or identical manner to the ones completed up to this point.